Journal of Medicinal Chemistry

Article

Acyclic nucleoside phosphonates containing a second phosphonate group are potent inhibitors of 6-oxopurine phosphoribosyltransferases and have antimalarial activity.

Dianne Therese Keough, Petr Špa#ek, Dana Hockova, Tomáš Tichý, Silvie Vrbková, Lenka Slav#tínská, Zlatko Janeba, Lieve Naesens, Michael D. Edstein, Marina Chavchich, Tzu Hsuan Wang, John de Jersey, and Luke W Guddat

J. Med. Chem., **Just Accepted Manuscript** • DOI: 10.1021/jm301893b • Publication Date (Web): 28 Feb 2013

Just Accepted

Acyclic nucleoside phosphonates containing a second phosphonate group are potent inhibitors of 6-oxopurine phosphoribosyltransferases and have antimalarial activity.

Dianne T. Keough[a], Petr Špaček[b], Dana Hocková[b*], Tomáš Tichý[b], Silvie Vrbková[b], Lenka Slavětínská[b], Zlatko Janeba[b], Lieve Naesens[c], Michael D. Edstein[d], Marina Chavchich[d], Tzu-Hsuan Wang[a], John de Jersey[a] and Luke W. Guddat[a*]

[a]The School of Chemistry and Molecular Biosciences, The University of Queensland, Brisbane, 4072, QLD, Australia; [b]Institute of Organic Chemistry and Biochemistry, Academy of Sciences of the Czech Republic, v.v.i. Flemingovo nám. 2, CZ-166 10 Prague 6, Czech Republic; [c]Rega Institute for Medical Research, KU Leuven, Minderbroedersstraat 10, B-3000, Leuven, Belgium; [d]Australian Army Malaria Institute, Enoggera, Brisbane, QLD 4051, Australia

ABSTRACT

Acyclic nucleoside phosphonates (ANPs) which contain a 6-oxopurine base are good inhibitors of the *Plasmodium falciparum* (*Pf*) and *Plasmodium vivax* (*Pv*) 6-oxopurine phosphoribosyltransferases (PRTs). Chemical modifications based on the crystal structure of 2-(phosphonoethoxy)ethyl-guanine (PEE-G) in complex with human HGPRT has led to the design of new ANPs. These novel compounds contain a second phosphonate group attached to the ANP scaffold. [(2-((Guanine-9*H*-yl)methyl)propane-1,3-diyl)bis(oxy)]bis(methylene))diphosphonic acid (compound **17**) exhibited a K_i value of 30 nM for human HGPRT and 70 nM for *Pf*HGXPRT. The crystal structure of this compound in complex with human HGPRT shows that it fills or partially fills three critical locations in the active site *i.e.* the binding sites of the purine base, the 5′-phosphate group and pyrophosphate. This is the first HG(X)PRT inhibitor that has been able to achieve this result. Prodrugs have been synthesized resulting in IC_{50} values as low as 3.8 μM for *Pf* grown in cell culture, up to 25-fold lower compared to the parent compounds.

Keywords: malaria, HGPRT, HGXPRT, prodrugs, crystal structure, purine salvage, phosphoribosyltransferase

Running Title: New ANPs have antimalarial activity

INTRODUCTION

Malaria remains one of the most important infectious diseases in the world today, affecting half of the world's population, with an estimated 216 million cases and reports of at least 655,000 fatalities in 2010.[1] Though there are five strains of *Plasmodium* that can infect humans, the most widespread and lethal are *falciparum* (*Pf*) and *vivax* (*Pv*).[2]

Resistance to the current drugs (including artemisinin based combination therapies) for treatment and prophylaxis of malaria is on the rise, underlining the need for the discovery of new drug targets and therapeutics.[3] One of the essential features required for long-term use of an effective chemotherapeutic is to target proteins/enzymes that would be difficult for the parasite to mutate without compromising its own ability to replicate. A second important criterion is the cost of synthesis of potential drugs. The purine salvage enzyme hypoxanthine-guanine-(xanthine) phosphoribosyltransferase (HG(X)PRT) and the acyclic nucleoside phosphonate (ANP) inhibitors are able to address both these factors. HG(X)PRT has long been recognized as a malarial drug target because its activity is essential for the synthesis of nucleoside monophosphates required for DNA/RNA production. **Figure 1** shows the reaction catalyzed by HG(X)PRT.

It has been shown that ANPs, which inhibit *Pf*HGXPRT, arrest parasite growth in cell culture.[4] Further, recent metabolic studies have confirmed that *Pf*HG(X)PRT activity is critical for the survival of *Pf* in cell culture. Most importantly, these studies demonstrated that potent inhibitors of this enzyme exert their ability to arrest the growth of *Pf* in cell culture via inhibition of the purine salvage pathway.[5] Genomic sequencing has suggested that, like *Pf*, *Pv* does not possess the enzymes necessary to

synthesize the purine ring *de novo* and it relies on the salvage pathway for the production of its purine nucleoside monophosphates.[6] Thus, it is hypothesized that inhibitors of *Pv*HGPRT will also be capable of arresting the growth of this parasite.

ANPs are cost-effective to produce. This is demonstrated by the fact that three prototype ANPs with an adenine or cytosine base are in use as antiviral drugs (tenofovir, adefovir and cidofovir)[7], with tenofovir being widely distributed to HIV-infected individuals in third world countries. The ability of these compounds to act as anti-viral agents is by inhibition of viral polymerases or reverse transcriptases after they have become phosphorylated by cellular kinases. Such compounds do not inhibit HG(X)PRT as neither pyrimidine bases nor purine bases containing a 6-amino group are recognized by this enzyme. New ANPs were then designed where the base is a 6-oxopurine so that they should specifically inhibit HG(X)PRT. Such compounds were subsequently found to selectively inhibit human HGPRT, *Pf*HG(X)PRT and *Pv*HGPRT[8], to arrest the *in vitro* growth of *Pf* cell lines and to have low cytotoxicity in mammalian cell lines.[4b] An important feature of the ANPs is that they contain a stable carbon-phosphorous bond so they cannot be hydrolysed in the cell to inactive derivatives. Schramm and colleagues have suggested that the reason why the transition state analogs, immucillin 5′-phosphates, cannot act as antimalarials is because of hydrolysis of this group by phosphomonoesterases.[5c] ANPs also possess a further desirable property and this is that they can be chemically modified to produce prodrugs to increase cell permeability.[9]

Previously, 9-(2-(phosphonoethoxy)ethyl)guanine (PEEG) or –hypoxanthine (PEEHx) (**Figure 2**), were found to be good and selective inhibitors of human HGPRT and *Pf*HGXPRT.[4b, 8a] The K_i values of PEEG for human HGPRT and *Pf*HGXPRT are 1.0 and 0.1 μM, respectively and, for PEEHx, are 3.6 and 0.3 μM. Crystal structures of

these two compounds in complex with human HGPRT suggested possibilities for the design of more potent inhibitors. One idea was to synthesize new compounds containing a second phosphonate group designed to occupy the PP_i binding pocket. Thus, previously synthesized bisphosphonates[10] as well as newly designed ANPs with a phosphonate group attached to the PEE, 2-(phosphonomethoxy)ethyl (PME) or 3-(phosphonomethoxy)propyl scaffold could be tested as inhibitors of HG(X)PRTs.

A series of lipophilic prodrugs of the ANP inhibitors were then synthesized and their IC_{50} values for the growth of *Pf* in cell culture determined. In parallel, the cytotoxicity of these compounds was measured in three different cell lines, *i.e.* human lung carcinoma cells, a human melanoma cell line and a derived HGPRT-deficient mutant cell line. The crystal structure of human HGPRT in complex with [[(2-((guanine-9*H*-yl)methyl)propane-1,3-diyl)bis(oxy)]bis(methylene))diphosphonic acid (compound **17**), which has the highest affinity for human HGPRT and *Pf*HGXPRT, shows how this class of ANPs bind in the active site.

RESULTS

Chemistry. The key branched hydroxyderivative **2** for the synthesis of unsymmetrical bisphosphonate type of ANPs (**Scheme 1**, compounds **7** and **8**) was prepared by the multistep sequence starting from racemic solketal.[11] For the introduction of the acyclic moiety to the N^9-position of 6-chloropurine or 2-amino-6-chloropurine the Mitsunobu reaction[12] was applied. The resulting 6-chloropurine bisphosphonate **3** was transformed to hypoxanthine derivative **5** by nucleophilic aromatic substitution in acidic conditions (75% aqueous trifluoroacetic acid). In the case of 2-amino-6-chloropurine bisphosphonate **4**, the Mitsunobu reaction had to be followed by heating in water/tetrahydrofuran to decompose the triphenylphosphoranylidene intermediate[13]

rising from the presence of the free amino group. The chlorine atom was next displaced with hydroxyl in quantitative yield as described above to form guanine derivative **6**. This two step approach for preparation of N^9-substituted hypoxanthine/guanine derivatives affords better results than the direct alkylation of 6-oxopurines complicated by the formation of N^7-regioisomers. To form free racemic bisphosphonic acids **7** and **8**, both phosphonate moieties of **5** and **6** were simultaneously deprotected under standard conditions using Me_3SiBr/acetonitrile followed by hydrolysis.

For the synthesis of symmetrical bisphosphonates **16** and **17,** the known precursor **11** was prepared. Although we have reported the variant synthesis of guanine derivative **17** previously,[10b] the above described synthetic approach for the unsymmetrical ANPs (including Mitsunobu reaction, followed by aromatic substitution and ester cleavage), is a new synthetic method (**Scheme 2**) for the preparation of the guanine bisphosphonate as well as the new hypoxanthine derivative **16**.

The tetraesters of bisphosphonates **5-6** and **14-15** were used for the direct preparation of the phosphoramidate prodrugs[9] **9-10** and **18-19** by our recently published method that is highly efficient.[14] In the first step of the one-pot reaction, sequence the deprotection of the phosphonate esters **5-6** and **14-15** with Me_3SiBr forms in situ the tetra(trimethylsilyl) esters. In the second step the reaction of these intermediates with ethyl (L)-phenylalanine in the presence of 2,2′-dithiodipyridine (Aldrithiol) and triphenylphosphine yield the corresponding tetra-amidates **9-10** (**Scheme 1**) and **18-19** (**Scheme 2**).

Inhibition of the human, *Plasmodium falciparum* and *Plasmodium vivax* 6-oxopurine PRTases.

A series of ANPs containing a second phosphonate group attached to the acyclic linker between the N^9 atom of the purine base and the first phosphonate group were synthesized, with the aim of increasing the potency for the 6-oxopurine PRTases (**Schemes 1** and **2**). In these structures, the second phosphonate group is attached either to the first or second carbon atom from N^9 of the purine base (**Figure 3**). The number of atoms between N^9 and the first phosphorus atom is 5 or 4, and between N^9 and the second phosphorus atom varies between 4 and 6. In compounds **17**, **16** and **20** (**Figure 3**), the oxygen atom is located in a different position compared with the PEE compounds shown in **Figure 2**. While in compounds **17**, **16** and **20** the bisphosphonate acyclic moiety is symmetric, compound **8** have different linkers connecting the first and the second phosphonate group. The K_i values for these compounds are given in **Table 1**.

Compound **17** (**Scheme 2**) is a potent inhibitor of the human and *Pf* enzymes. The attachment of a second phosphonate group results in a 33-fold decrease in K_i value for human HGPRT but only a 1.5-fold decrease for *Pf*HGPRT compared with PEEG.[4b, 8a] Although this compound is an excellent inhibitor of these two enzymes, it is not as effective against *Pv*HGPRT (**Table 1**). The biggest decrease in K_i for this compound occurs for the human enzyme and, thus, the attachment of this second group is accompanied by a loss in selectivity.

Human HGPRT and *Pf*HGXPRT have 48% amino acid sequence identity. There are only two published structures of *Pf*HGXPRT.[5c, 15] Comparison of these crystal structures with those of human HGPRT show that the residues whose side-chains that

enter the active site are all identical.[16] However, the active sites contain several flexible loops that can change their conformation depending on the inhibitor that is bound. These changes contribute to the K_i values. It has been demonstrated that selectivity does exist between the enzymes. This is based on the fact that purine bases with simple atomic substitutions have different K_m values.[17] It This is one avenue that can be explored to increase selectivity. Furthermore, other ANPs can also exhibit selectivity.[4b, 5c, 8e] The attachment of a second phosphonate group decreases the K_i values[8e] as predicted from modelling but such compounds bind to human HGPRT and *Pf*HGPRT with similar affinities. The selectivity issue can only be addressed by further crystal structures of *Pf*HGXPRT in complex with ANPs containing a second phosphonate group.

Compound **16** (**Scheme 2**), with hypoxanthine instead of guanine as the purine base, has a higher K_i value for all three enzymes, compared with compound **17**. This difference is 33-fold for human HGPRT, 71-fold for *Pf*HGXPRT and 3-fold for *Pv*HGPRT (**Table 1**). In comparison, PEEG also binds more tightly to the human and *Pf* enzymes than PEEHx, but in this case the difference between the guanine and hypoxanthine analogues is only 3-fold.[4b, 8a] Thus, for these bifunctional ANPs, the nature of the purine base makes a marked contribution to the affinity.

Compound **8** (**Scheme 2**), with guanine as the base, has a decreased affinity for the human and *Pf* enzymes compared with compound **17**. This could be attributed to one or both of two factors: (i) the phosphonate group which binds in the 5′-phosphate binding pocket is too long for optimal interactions; and/or (ii) it is the positioning of the oxygen atom in the linker in the second phosphonate tail that influences affinity. For *Pv*HGPRT, neither of these factors has any effect as the K_i is the same for

compound **17** and compound **8**. In this series, compound **8** is the only one with similar affinity for all three enzymes.

Compound **20** is a weak inhibitor of the human HGPRT and, though not a potent inhibitor of the two parasite enzymes, it prefers *Pf*HGXPRT and *Pv*HGPRT (**Table 1**). Compound **20** is a derivative of 2-(phosphonomethoxy)ethyl guanine (PMEG). PMEG inhibits the human and *Pf* enzymes with similar K_i values to those found for compound **20**, *i.e.* 29 μM for human HGPRT and 1.6 μM for *Pf*HGXPRT.[4b] Therefore, it is unlikely that, in this instance, the second phosphonate group makes interactions with any amino acids in the active site and, therefore, does not contribute to the affinity of these ANPs for the enzymes.

*Crystal structure of [(2-((guanine-9H-*yl*)methyl)propane-1,3-diyl)bis(oxy)]bis(methylene))diphosphonic acid* (*compound **17**) in complex with human HGPRT*

The crystal structure of compound **17** in complex with human HGPRT has been determined to 2.0 Å resolution, with the asymmetric unit constituting a human HGPRT tetramer (**Figure 4a**; **Table 2**).

The electron density map in **Figure 4b** exemplifies that each active site is occupied by a single molecule of compound **17**, a sulfate ion (from the crystallization buffer) and two magnesium ions. Superimposition of the four subunits shows that the purine ring, the two phosphonate groups, the sulfate ion and the two magnesium ions align with a high degree of precision (rmsd for all atoms < 0.2 Å). Thus, the purine ring and the two phosphonate groups are firmly held in place. However, due to the free rotation of the dihedral angles within the linker regions, there is variability in the location of these atoms with differences in the atomic coordinates of up to 1.4 Å.

*Factors that influence the tight binding of compound **17***

There are a number of factors that contribute to holding compound **17** in the active site. These are: (i) the purine base; (ii) the phosphonate group mimicking the 5′-phosphate group of *P*Rib-*PP* or GMP; (iii) the second phosphonate group (attached to the linker connecting the purine base to the phosphonate group) mimicking pyrophosphate; (iv) the chemical nature of each of the two acyclic linkers; and (v) the presence or absence of divalent metal ions in the active site. These are discussed below.

Purine binding site

The purine base of compound **17** slots under the aromatic ring of F186 forming a Π stacking interaction. This arrangement occurs in all the published structures of the 6-oxopurine PRTases when a compound containing a purine base is bound. Four hydrogen bonds contribute to the binding of compound **17**. These are between (i) the 6-oxo group of the guanine base and the NZ atom of K165; (ii) N^7 of the guanine base with NZ of K165; (iii) the 6-oxo group of the guanine base and the backbone amide of V187; and (iv) the amino group of the guanine base with the carbonyl group of D193. The formation of bond (iv) is a likely reason why the replacement of guanine by hypoxanthine increases the K_i by ~30-fold as this interaction cannot be made when a hydrogen is substituted for the exocyclic amino group.

5′-phosphate binding site

The first phosphonate group of symmetric compound **17** is designed to reach into the 5′-phosphate binding pocket in a similar way as the 5′-phosphate group of *P*Rib-*PP* or GMP. This pocket is defined by residues 137-141 which encircle this group (**Figure 4c**). This phosphonate group contributes to the affinity of ANPs for these enzymes and

is essential for tight binding. When compound **17** is bound, a network of hydrogen bonds between the main-chain nitrogen atoms of D137, G139, T141 and the hydroxyl groups of T138 and T141 and the oxygen atoms of the phosphonate group is formed (**Figure 4c**).

Binding site of the second phosphonate group

The second phosphonate group of compound **17** points down into the vicinity of the PP_i binding pocket (**Figure 4c**). When binding occurs, the backbone dihedral angles for K68 rotate such that the side chain of this amino acid residue rotates away from the active site by 180° (**Figure 4d**) and occupies the same position as when the transition state analog, ImmGP and $Mg^{2+}.PP_i$ are bound.[18] The NZ atom of K68 in the human HGPRT.compound **17** complex then forms a hydrogen bond with the carbonyl group of V96 in an adjacent subunit. In the absence of the second phosphonate group *i.e.* when PEEG or PEEHx are bound, K68 occupies the same location as PP_i and is pointed upwards towards the PEE scaffold.[4b] The phosphoryl oxygen atoms of this phosphonate group in compound **17** are anchored in position by Mg^{2+} and via this ion to the side chain of D193. This appears to be an important interaction that contributes to the tighter binding of compound **17** compared with PEEG.

With the rotation of the side chain of K68, this area of the enzyme is then solvent accessible and a sulfate ion, present in the crystallization solution, is able to enter the active site. The sulfate ion is located in the same position as one of the phosphate groups of PP_i when it is bound together with the transition state analog.[18] Its interactions with the active site residues are therefore similar to that of the phosphoryl oxygen atoms of one of the phosphate groups in PP_i. It is unlikely that the presence of sulfate ions effects either the location or affinity of compound **17**. This interpretation is

based on the observation that the addition of sulfate ions to the assay did not result in a decrease in K_i value for compound **17**.

*Magnesium ions in the structure of the human HGPRT.*compound **17** *complex*

It has been hypothesized that magnesium ions bind to *P*Rib-*PP* prior to this substrate entering the active site. Human HGPRT obeys a sequential mechanism with *P*Rib-*PP* binding first, followed by the purine base. PP_i then leaves followed by the nucleoside monophosphate product, whose release is the rate-limiting step.[19] The catalytic mechanism of the two *Plasmodium* enzymes has not been determined. However, it is assumed that they follow the same reaction pathway though this may not necessarily be the case. There are no divalent metal ions present in the crystal structure of free human HGPRT[20] or when it is in complex with GMP[16] or IMP. However, two magnesium ions are located in the active site when the transition state analog, ImmGP, and PP_i are bound. One magnesium ion is bound to the two hydroxyl groups of the ribose ring and to two oxygen atoms of pyrophosphate, while the second is coordinated to two oxygen atoms of pyrophosphate and to the OD1 atom of D193.[18]

In the human HGPRT.compound **17** complex, one magnesium ion is bound to the phosphonate group located close to the PP_i binding site as described above. The second is bound to a carboxylate oxygen atom of E133 (2.1 Å) and to the OD1 atom of D134 (2.1 Å). This is a different arrangement from that found when ImmGP.Mg^{2+}.PP_i[18] is bound. In that instance, there are no direct interactions with either of these side chains and magnesium ion is only linked to the side chain of E133 via a water molecule. It is unclear if, in some of the 6-oxopurine PRTases, magnesium ions bind independently before the substrates enter. It has been proposed that, if the unliganded enzyme is found to contain Mg^{2+}, then the role of these ions may be to help to stabilize the active

site so that the catalytic reaction can proceed.[21] Magnesium ions have been observed in crystal structures of the two *E. coli* 6-oxopurine PRTases in the absence of ligands.[21] In *E. coli* XGPRT, this divalent metal ion is stabilized by bonds to surrounding water residues and to the OD1 atom of D89 and in *E. coli* HPRT to the side chain atoms of E103 and D104. The corresponding residues in human HGPRT are E133 and D134. In the crystal structures of human HGPRT in complex with three different ANPs, *i.e.* 2-(phosphonoethoxy)ethyl- guanine or -hypoxanthine (PEEG and PEEHx) and (*S*)-3-hydroxy-2-(phosphonomethoxy)propyl guanine [(*S*)-(HPMPG)],[4b] no divalent metal ions were found in the active site. This may be because these compounds more closely mimic that of the nucleoside monophosphate product of the reaction. Thus, it is only when in complex with the ANP, compound **17**, that two divalent metal ions have become coordinated. The role of this second ion in human HGPRT in complex with this inhibitor may well be to shape the active site to allow for tighter binding.

In vitro *antimalarial activity and cytotoxicity studies*

In order to increase cell permeability, the negative charges on the ANPs may need to be masked. One approach is to attach hydrophobic or lipophilic groups to the parent ANP by an ester or phosphoramidate bond. The concept for these delivery systems and the ability to be hydrolysed enzymatically *in vivo* to the active compound is based on the previous experiences with related ANPs that are anti-viral drugs.[9] Initially, prodrugs of PEEG (**Figure 2**) were synthesized.[22] As shown in **Figure 5**, compound **21** contains two phosphoramidate moieties, whereas the other two prodrugs contain one (compound **23**) or two (compound **22**) hexadecyloxypropyl chains. The IC_{50} values for the prodrugs of PEEG in the chloroquine-sensitive and the chloroquine-resistant strains are given in **Table 3**. The cytostatic concentrations were determined in three human cell lines (**Table 3**).

The prodrugs all have lower IC_{50} values compared to PEEG against *Pf* cell lines. The most active prodrug (compound **23**) has a single lipophilic chain attached to the phosphonate group. However, this compound is also the most toxic in mammalian cell lines. Addition of the second lipophilic group (compound **22**) reduces the antimalarial activity compared to the single prodrug, but this compound is still considerably more active than PEEG. It has been demonstrated that intracellular cleavage of hexadecyloxypropyl prodrugs of ANPs is performed by phospholipase C.[23] The lower activity of the double, compared to the single ester prodrug, is consistent with a previous report.[22a] This may be attributed to the fact that either the phosphonate double-ester prodrug penetrates the cell membrane less rapidly than its monoester counterpart or that the monoester is hydrolyzed more rapidly once inside the cell to the active ANP or, perhaps, a combination of both these factors.[23]

Highly polar bisphosphonates (such as compounds **17**, **16**, **8** and **20**; **Figure 3**) are unable to cross the cell membranes. A phosphoramidate type of prodrug was therefore synthesized to try to increase their antimalarial activity. Since the alanine-based phosphoramidate compound **21** (**Table 3**) was not as successful as compound **23** (**Table 3**), the more hydrophobic ethyl (L)-phenylalanine was used to mask all four hydroxy groups (**Figure 6**).[24] The results of the *in vitro* antimalarial activity and cytotoxicity of the tetraphosphoramidates are given in **Table 4**.

The prodrugs are effective in inhibiting parasite growth with a decrease in the IC_{50} value of at least 100-fold compared with compound **17**. Compound **18** containing hypoxanthine as the base is slightly more effective than when guanine is the base (compound **19**). However, it is more cytotoxic in mammalian cells. Compound **10** has similar cytotoxic properties as compound **18**. Though these compounds are slightly better inhibitors of *Pf*HGXPRT compared with PEEG (K_i = 0.1 μM), the *in vitro* data

suggests that the efficient design of prodrugs, leading to good cell permeability and efficient hydrolysis within the cell are important factors to be considered in drug design. The corresponding prodrug of the bisphosphonate compound **20** was not synthesized for cell based asays. This is because compound **20** has similar K_i values as PMEG, the compound on which it was modeled. PMEG has an IC_{50} value against *Pf* cell lines (14 μM), but its CC_{50} in mammalian cells is 17 μM, resulting in a low SI value.[4b]

Discussion

One of the new bifunctional ANPs, compound **17**, has a K_i of 30 nM for human HGPRT, 70 nM for *Pf*HGXPRT and 600 nM for *Pv*HGPRT. The crystal structure of compound **17** in complex with human HGPRT shows that this second phosphonate group is located in the vicinity of the PP_i binding pocket (**Figure 4c**). It is held in position by interactions with a magnesium ion (2.1 Å) and, through this, to the carboxylate group of D193 (2.1 Å). This is the only interaction that this group forms with active site amino acid residues and is a critical contribution to its low K_i value. In the human HGPRT.compound **17** complex, the side chain of K68 has moved from its location found in the free structure or in the human.GMP complex.[16] This movement results in the PP_i binding site becoming vacant, making room for sulfate to enter the active site. It could be argued that the reverse situation occurs and that sulfate binds first, allowing compound **17** to bind. However, the addition of either sulfate or phosphate has no effect on the K_i for compound **17**, making this an unlikely proposition. The sulfate ion is located in precisely the same position as one of the phosphate groups of pyrophosphate when PP_i is bound in the active site together with ImmGP and Mg^{2+}. One of the sulfate oxygen atoms forms interactions with Mg^{2+} (2.2 Å) and the OD1 of D193 (2.9 Å) while the other is now 2.9 Å from the amide nitrogen

of K68. The only interaction with the phosphonate group of compound **17** is through the same magnesium ion (**Figures 4c** and **4d**). Thus, though the presence of sulfate in the active site is a result of its presence in the crystallization buffer and does not itself contribute to the binding of compound **17**, its location does suggest chemical modifications to compound **17** to increase its potency.

There is also a second magnesium ion present in the human HGPRT.compound **17** complex. This is bound to the carboxylate side chains of E133 and D134. Though the rationale for the presence of this magnesium ion is not fully understood, it can be speculated that its presence may help to shape the active site allowing compound **17** to bind in its optimal position.

If the phosphonate group is attached one atom closer to the N^9 atom as in compound **20**[10b] (**Figure 3**), there is no change in the K_i value compared with PMEG on which this ANP was based. This suggests that, in this case, the second phosphonate group is too close to N^9 and cannot bind in the vicinity of pyrophosphate. Thus, the interactions between PMEG and compound **20** with active site residues are identical irrespective of whether the second phosphonate moiety is attached or not. This accounts for the fact that there is no change in the K_i value for either the human or *Pf* enzymes.

The K_i value for compound **17** for human HGPRT is 33-fold lower than for PEEG. However, there is not such a large difference between the K_i values for compound **17** and PEEG for *Pf*HGXPRT (1.5-fold). This suggests that the interactions between compound **17** and human HGPRT which contribute to the high affinity may be slightly different from those that occur when compound **17** binds to *Pf*HGXPRT. One likely explanation is that magnesium ions do not bind to *Pf*HGXPRT in the presence of compound **17**. Though the free structure of human HGPRT does not contain metal

ions, they are always present in the storage buffer and appear to be necessary for this enzyme to maintain its maximum activity. In comparison, *Pf*HGXPRT does not require metal ions to maintain its structure. This enzyme is stable for at least 24 months as long as *P*Rib-*PP* and hypoxanthine are present. Indeed, totally inactive *Pf*HGXPRT, which occurs during the purification in the absence of Mg^{2+}, *P*Rib-*PP* and hypoxanthine, can be restored to full activity by adding these two substrates in the absence of divalent metal ions to the inactive enzyme. For *Pf*HGXPRT, divalent metal ions may only be important in catalysis. It is conceivable that compound **17** binds to *Pf*HGXPRT in the absence of metal ions and that the interaction between the active site residues in human HGPRT (carboxylate group of D193), the second phosphonate group and $Mg^{2+,}$ cannot occur. Hence, there is no dramatic reduction in the K_i values for PEEG and compound **17** with *Pf*HGXPRT. There are two published structures of *Pf*HGXPRT but, in both cases, $Mg^{2+}.PP_i$ is present.[5c, 15] As PP_i should bind only in the presence of a divalent metal ion, the structure of *Pf*HGXPRT.compound **17** is required to determine if compound **17** can bind in their absence. An explanation for the slightly higher K_i for compound **17** with *Pv*HGPRT compared with the human and *Pf* enzymes cannot be advanced as the structure of this enzyme is presently unknown.

The other change in the chemical structures of compound **17** and compound **16** (**Figure 3**) compared with the PEE moiety is isosteric. In these new inhibitors, the oxygen is moved to a different position in the linker connecting the N^9 atom of the purine ring to the phosphonate group binding in the 5′-phosphate pocket. This change alters the shape of the linker so that there is one more hydrogen bond between the phosphoryl oxygen atoms with the amino acid residues (137-141) for compound **17** than for PEEG. This is between the amide nitrogen atom of T138 and the oxygen atom (O1) that forms bonds with the amide atom of D137 and G139. There are also closer

interactions between the phosphoryl oxygen atoms of O2 and O3 and the active site amino acid residues for compound **17** than for PEEG. The bond between O2 and the carboxyl oxygen atom of T141 is slightly tighter for compound **17** compared with PEEG (2.4-2.7 Å for compound **17** and 2.6-2.8 Å for PEEG). The O3 atom of compound **17** and the amide nitrogen of T138 forms a closer interaction than in the human.PEEG complex (2.6-2.9 Å compared with 2.9-3.14 Å). There is also a tighter interaction between O3 and the carbonyl atom of T138 (2.4-2.8 Å compared with 2.8-3.0 Å). Thus, these tighter interactions found for compound **17** are another factor contributing to its affinity.

There are four amino acid side chains or backbone atoms that have been found to form hydrogen bonds to guanine. These are the carbonyl group of V187, the OD1 atom of D193, the NZ atom of K165 and the OD1 atom of D137. In the purine base, four atoms are capable of forming hydrogen bonds to these active site residues (N^1, exocyclic amino group at position 2, exocyclic atom at position 6 and N^7). However, this constellation of hydrogen bonds differs in the structures of human HGPRT in complex with these two different ANPs, PEEG and compound **17**. In complex with compound **17**, there is a hydrogen bond between the 2-amino group of guanine with the carbonyl atom of D193 (2.9-3 Å). This does not occur when PEEG binds as it is too far away (3.5-4 Å). The exocyclic atom in the 6-position of the purine base also form a weaker interaction with the amide nitrogen of V187 for PEEG (*cf.* 2.8 -2.9 Å for compound **17** with 3.0-3.5 Å for PEEG). The NZ atom of K165 forms a hydrogen bond with the N^7 atom of the purine ring when compound **17** binds (2.5-2.7 Å). However, this hydrogen bond is absent in the human.PEEG complex (3.2-3.5 Å). Thus, the nature of the linker is an important contributing factor in determining the optimal orientation and location

of the purine base and the phosphonate group which binds in the 5′-phosphate binding pocket.

There are subtle differences in the binding of guanine in the active site depending on the chemical nature of the attachment to the base.[4b, 16, 18] However, there are always two common interactions with the active site amino acid residues: (i) a hydrogen bond between the N^1 atom with the carbonyl oxygen of V187; and (ii) a hydrogen bond between the 6-oxo group with the NZ atom of K165. The differences lie in the interactions of the 2-amino group and the N^7 proton. The 2-amino group in compound **17** is able to form two hydrogen bonds with active site residues though, in the case of PEEG, only one such bond occurs. For the immucillins, PEE and other ANP derivatives, human HGPRT has higher affinity for the compounds containing guanine instead of hypoxanthine. The exception is IMP and GMP where there is little difference in the K_i value.[17] It is clear that the loss of hydrogen bonds when the exocyclic amino group is replaced by a proton would result in a decrease in affinity. However, this alone is not sufficient to explain the fact that, for the PEEG and PEEHx, this difference is only 4-fold while, for compound **17** and compound **16** (**Table 1**), this difference is 33-fold. The structures of four inhibitors containing guanine as the base (ImmGP, GMP, PEEG and compound **17**) in complex with human HGPRT show that there are subtle differences between these structures in the binding of the base. For example, the N^7 atom in compound **17** forms a hydrogen bond with the NZ atom of K165. This does not occur when GMP or ImmGP are bound. The N^7 atom of ImmGP rather forms a hydrogen bond with the carboxyl atom of D137 while, in the GMP complex, N^7 does not form a hydrogen bond to any of the atoms in the active site. Another difference in binding is the hydrogen bond between the 6-oxo group in compound **17** and the amide nitrogen of V187. Such a hydrogen bond cannot form for

PEEG, ImmGP or GMP. Thus, one possibility to explain the differences in affinity between compound **17** and compound **16** (**Table 1**) is that, when hypoxanthine replaces guanine, there is a subtle difference in the binding of this base weakening the interactions with the enzyme.

The attachment of lipophilic groups through an ester or phosphoramidate bond leads to a reduction in IC_{50} of the prodrugs when compared with the active ANPs (**Tables 3** and **4**). The ability of the ANP prodrugs in erythrocyte cultures to act as anti-malarials can be attributed to their first being able to enter the cells and their subsequent hydrolysis within the cells by inherent enzymes. Whether the hydrolysis of the produg occurs within the red blood cell and it is the ANP that enters the parasite, or, whether it is the prodrug that is transported and then hydrolysed within the parasite itself, is at present unknown. Also unknown is the resultant concentration of the active compound within the parasite. These factors are currently being addressed and should lead to the design of more effective anti-malarials.

Compounds **21** and **22** (**Table 3**) and the compound **17** (**Tables 1** and **4**) have little, if any cytostatic effects in the A549, in the C32 and C32TG cell lines. The prodrug of compound **17** (compound **19**, **Table 4**) also has low though detectable cytotoxicity values in C32 and C32TG cell lines. It is hypothesized that these cytotstatic values are not because these prodrugs cannot enter the mammalian cells. This is based on the fact that they must have traversed this barrier to reach their parasitic target. There are two pieces of evidence that suggest that those compounds (compound **23**, **Table 3** and compounds **18** and **10**, **Table 4**) which are slightly cytostatic do not exert these effects by inhibition of human HGPRT activity. The first is that compound **17** (**Table 1**) has the lowest K_i value of all the ANPs for human HGPRT (0.03 μM) while the parent compounds of **18** and **10** (**16** and **8**, **Table 1**) have higher K_i values of 1 and 0.6 μM,

respectively. Thus, if inhibition of human HGPRT was the cause of the cytotoxicity, then compound **17** (and its prodrug 19) would be expected to have the higher CC_{50} value. The second piece of evidence is there is no difference in the CC_{50} values for these compounds between C32 and C32TG. As C32TG cannot express HGPRT activity, it would be expected to have lower cytotoxicity values than in C32 if human HGPRT was the target. The explanation for the weak though measurable cytotoxicity is complicated by the fact that these cells have a high proliferation rate with a very active pathway of *de novo* purine biosynthesis. A549 cells have a higher rate of proliferation than the C32 and C32TG cells, which may make them less sensitive. One possible suggestion to explain the cytostatic properties is that certain ANPs can be converted to toxic metabolites by enzymes such as kinases present within the cell.

In conclusion, a new potent inhibitor (compound **17**) of the 6-oxopurine PRTases has been discovered. The crystal structure of compound **17** in complex with human HGPRT has suggested reasons for the affinity for human HGPRT and possible explanations for the affinity for *Pf*HGXPRT. This structure opens possibilities for the design of even more potent inhibitors. Chemical modifications whereby hydrophobic groups are linked to this compound via a phosphoramidate bonds result in an increase in the ability to arrest parasitic growth. The prodrug of compound **17** (compound **19**) has little, if any, cytostastic properties in the mammalian cell line, A549. This data suggests that compound **17** is a promising lead compound for further development to increase its antimalarial efficacy.

EXPERIMENTAL SECTION

Synthesis and Analytical Chemistry. Unless otherwise stated, solvents were evaporated at 40 °C/2 kPa, and the compounds were dried over P_2O_5 at 2 kPa. NMR spectra were recorded on Bruker Avance 500 (^{1}H at 500 MHz, ^{13}C at 125.8 MHz),

Bruker Avance 600 (^{1}H at 600 MHz, ^{13}C at 151 MHz) and Bruker Avance 400 (^{1}H at 400 MHz, ^{13}C at 100.6 MHz) spectrometers with TMS as internal standard or referenced to the residual solvent signal. Mass spectra were measured on a ZAB-EQ (VG Analytical) spectrometer. The purity of the tested compounds was determined by the combustion analysis (C, H, N) and was higher than 95%. The chemicals were obtained from commercial sources or prepared according to the published procedures. THF was distilled from sodium/benzophenone under argon. Unless otherwise stated, preparative HPLC purifications were performed on columns packed with 7 μm C18 reversed phase resin (Waters Delta 600 chromatograph column), 17 × 250 mm; in ca. 200 mg batches of mixtures using gradient MeOH/H_2O as eluent.

Synthesis of the ANPs

Tetraethyl ([(3-(hydroxy)propane-1,2-diyl)bis(oxy)]bis(ethylene))bis(phosphonate) (2)

Solketal (20.8g, 157.4 mmol) was transform to 4-((benzyloxy)methyl)-2,2-dimethyl-1,3-dioxolane by the known procedure[11b] (yield 33.8 g). Then methanol-water (10:1, 1100 ml) and DOWEX (50x8; 80 g) was added and the reaction mixture was refluxed for 4 h.[11a] The DOWEX was removed by filtration. The solvent was evaoprated *in vacuo* and the residue was co-distilled with toluene (2x). The resulting crude 3-(benzyloxy)propane-1,2-diol (25.8 g, presence was confirmed by GC-MS) was used without purification to the next step: To a well suspended mixture of 3-(benzyloxy)propane-1,2-diol (9.1 g) and Cs_2CO_3 (16.3 g. 49.8 mmol) in *tert*-BuOH (52.5 ml) under argon, diethyl vinylphosphonate (24 ml, 155 mmol) was added.[11c] The reaction mixture was stirred at RT for 5 days. The resulting mixture was poured to the water (200 ml) and extracted by EtOAc (2 x 200 ml). Organic layers were collected

and washed by water (2 x 200 ml) and brine (1 x 200 ml) and dried with $MgSO_4$. Solvent was evaporated *in vacuo* and residue (29.18 g) was used without purification to the next step. Part of this crude tetraethyl ([(3-(benzyloxy)propane-1,2-diyl)bis(oxy)]bis(ethylene))bis(phosphonate) (**1**, 5.9 g) was purified by flash chromatography ($CHCl_3$:MeOH; gradient 0.5-5 %) for determining the NMR spectra and UPLC-MS.

A solution of intermediate **1** (23.3 g) in MeOH (480 ml) containing a catalytic amount of $PdCl_2$ in HCl (aq) was hydrogenated over 10% Pd/C (2.2 g) at room temperature overnight. The suspension was filtered over Celite and washed with methanol (50 ml) and the filtrate was made alkaline by triethylamine. The solvent was evaporated *in vacuo* and the residue was purified by flash chromatography ($CHCl_3$:MeOH; gradient 1-6%) to give **2** (11 g) as colourless oil. The overall yield (from solketal) was 23.5%. ^{1}H NMR (DMSO-d_6): 4.63 bt, 1 H, J(OH,1') = 5.6 (OH); 3.93-4.04 m, 8 H (Et); 3.64-3.79 m, 2 H (H-6'); 3.54-3.60 m, 2 H (H-4'); 3.35-3.47 m, 5 H (H-1' and H-2' and H-3'); 1.98-2.08 m, 4 H (H-5' and H-7'); 1.22 t, 12 H, J(CH_2 , CH_3) = 7.0 (Et). ^{13}C NMR (DMSO-d_6): 79.54 (C-2'); 70.34 (C-3'); 64.87 d, J(C,P) = 1.2 (C-4'); 63.62 d, J(C,P) = 1.0 (C-6'); 61.17 and 61.14 and 61.12 d, J(C,P) = 6.2 (Et_3); 60.88 (C-1'); 26.61 d, J(C,P) = 136.6 (C-7'); 26.14 d, J(C,P) = 137.0 (C-5'); 16.43 d, J(C,P) = 5.8 (Et). MS (ESI): m/z = 511.3 $[M+H]^+$.

Tetraisopropyl ([(2-(hydroxymethyl)propane-1,3-diyl)bis(oxy)]bis(methylene))bis(phosphonate) (11)

Hydroxyderivative **11** was prepared according the known procedure.[10a]

Synthesis of 6-chloropurine derivates 3 and 12 via Mitsunobu reaction - General procedure

To a solution of triphenylphosphine (5.62 g, 21.4 mmol) in dry THF (75 ml) cooled to –30 °C under argon atmosphere diisopropylazadicarboxylate (DIAD, 3.9 ml, 19.8 mmol) was added. The mixture was stirred for 30 min to preformed complex. The solution of alcohol **2** or **11** (6.42 mmol) in THF (50 ml) and the 6-chloropurine (1.6 g, 10.4 mmol) was added to the preformed complex and reaction flask was filled with argon again. The resulting mixture was slowly warmed to room temperature and stirred twice overnight. Solvent was evaporated and the crude mixture was purified by flash-chromatography (silicagel, eluent $CHCl_3$:MeOH, gradient). Pure product was obtained as yellowish solid.

Diethyl (2-(3-(6-chloro-9*H*-purin-9-yl)-2-(2-(diethoxyphosphoryl)ethoxy)propoxy)ethyl)phosphonate (**3**): starting from hydroxyderivative **2**, yield 64%. ^{1}H NMR (DMSO-d_6): 8.79 s, 1 H (H-2); 8.68 s, 1 H (H-8); 4.49 dd, 1 H, *J*(gem) = 14.4, *J*(1'b, 2') = 4.1 (H-1'b); 4.36 dd, 1 H, *J*(gem) = 14.4, *J*(1'a, 2') = 7.0 (H-1'b); 3.85-4.05 m, 9 H (Et and H-2'); 3.67 m, 1 H (H-6'b); 3.53-3.61 m, 2 H (H-4'); 3.52 m, 1 H (H-6'a); 3.42-3.46 m (3'); 2.04 dt, 2 H, *J*(5',P) = 18.3, *J*(5',4') = 7.3 (H-5'); 1.89 dt, 2 H, *J*(7',P) = 18.3, *J*(7',6') = 7.4 (H-7'); 1.22 t and 1.171 t and 1.170 t, 12 H, *J* = 7.1 (Et). ^{13}C NMR (DMSO-d_6): 152.45 (C-4); 151.67 (C-2); 149.10 (C-6); 148.39 (C-8); 130.79 (C-5); 75.92 (C-2'); 69.54 (C-3'); 65.03 d, *J*(C,P) = 1.2 (C-4'); 63.90 d, *J*(C,P) = 0.7 (C-6'); 61.19 d and 61.17 d and 61.15 d, *J*(C,P) = 6.2 (Et); 44.76 (C-1'); 26.33 d, *J*(C,P) = 136.8 (C-7'); 26.00 d, *J*(C,P) = 136.8 (C-5'); 16.45 d and 16.40 d and 16.39 d, *J*(C,P) = 5.8 (Et). MS (ESI): m/z = 557.1 $[M+H]^+$.

Tetraisopropyl ([(2-((6-chloro-9H-purin-9-yl)methyl)propane-1,3-diyl)bis(oxy)]bis(methylene))bis(phosphonate) (**12**): starting from hydroxyderivative **11**, yield 60%. ^{1}H NMR (DMSO-d_6): 8.77 s, 1 H (H-2); 8.67 s, 1 H (H-8); 4.58 dsept,

4 H, *J*(CH,P) = 7.7, *J* = 6.2 (*i*Pr); 4.34 d, 2 H, *J*(1',2') = 7.0 (H-1'); 3.71 dd, 2 H, *J*(gem) = 14.0, *J*(4'b,P) = 8.0 (H-4'b); 3.68 dd, 2 H, *J*(gem) = 14.0, *J*(4'a,P) = 8.0 (H-4'a); 3.53 dd, 2 H, *J*(gem) = 9.8, *J*(3'b,2') = 5.6 (H-3'b); 3.50 dd, 2 H, *J*(gem) = 9.8, *J*(3'a,2') = 5.8 (H-3'a); 2.57 tpent, 1 H, *J*(2',1') = 7.0, *J*(2',3'a) = *J*(2',3'b) = 5.7 (H-2'); 1.23 d and 1.22 d and 1.21 d, 24 H, *J* = 6.2 (*i*Pr). ^{13}C NMR (DMSO-d_6): 152.40 (C-4); 151.66 (C-2); 149.14 (C-6); 148.09 (C-8); 131.01 (C-5); 71.09 d, *J*(C,P) = 11.0 (C-3'); 70.36 d and 70.34 d, *J*(C,P) = 6.4 (*i*Pr); 65.28 d, *J*(C,P) = 164.2 (C-4'); 43.11 (C-1'); 39.24 (C-2'); 24.00 d and 23.91 d, *J*(C,P) = 3.8 and 4.5 (*i*Pr). MS (ESI): m/z = 599.3 $[M+H]^+$.

Synthesis of 2-amino-6-chloropurine derivates 4 and 13 via Mitsunobu reaction - General procedure

Starting from 2-amino-6-chloropurine and hydroxyderivatives 2 and 11 the procedure was identical as described above for 6-chloropurine. Then after the stirring of reaction mixture for twice overnight, water (100 ml) was added and the mixture was heated at 70 ^{o}C for 4 days. Solvent was evaporated and the residue was codistilled with toluen (3x) and purified by flash-chromatography (silica gel, eluent $CHCl_3$: MeOH, gradient). Pure product was obtained as yellowish solid.

Diethyl (2-(3-(2-amino-6-chloro-9H-purin-9-yl)-2-(2-(diethoxyphosphoryl)ethoxy)propoxy) ethyl)phosphonate (**4**): starting from hydroxyderivative **2**, yield 76%. ^{1}H NMR (DMSO-d_6): 8.23 s, 1 H (H-8); 7.05 bs, 2 H (NH_2); 4.35 dd, 1 H, J(gem) = 14.4, J(1'b, 2') = 4.1 (H-1'b); 4.22 dd, 1 H, J(gem) = 14.4, J(1'b, 2') = 7.1 (H-1'b); 4.01-4.17 m, 8 H (Et); 3.98 m, 1 H (H-2'); 3.78 m, 1 H, (H-6'b); 3.69-3.75 m, 2 H (H-4'); 3.66 m, 1 H (H-6'a); 3.54 m, 2 H (H-3'); 2.19 dt, 2 H, J(5',P) = 18.2, J(5', 4') = 7.3 (H-5'); 2.02 m, 2 H (H-7'); 1.35 t and 1.31 t, 12 H, *J* =

7.1(Et). ^{13}C NMR (DMSO-d6): 159.97 (C-2); 154.55 (C-4); 149.44 (C-6); 144.09 (C-8); 123.24 (C-5); 75.95 (C-2'); 69.62 (C-3'); 65.01 (C-4'); 63.87 (C-6'); 61.21 d and 61.19 d and 61.17 d and 61.16 d, J(C,P) = 6.2 (Et); 44.02 (C-1'); 26.35 d, J(C,P) = 136.4 (C-7'); 25.97 d, J(C,P) = 137.0 (C-5'); 16.44 d and 16.38 d, J(C,P) = 5.8 (Et). MS (ESI): m/z = 572.2 $[M+H]^+$.

Tetraisopropyl ([(2-((2-amino-6-chloro-9H-purin-9-yl)methyl)propane-1,3-diyl)bis(oxy)]bis(methylene))bis(phosphonate) (**13**): starting from hydroxyderivative **11**, yield 73%. The spectral data were in accord with the literature.[10a]

Synthesis of 6-oxopurine derivates 5-6 and 14-15 - General procedure

The 6-chloropurine or 2-amino-6-chloro purine derivative (**3, 12** or **4, 13**; 4.13 mmol) was dissolved in aqueous trifluoroacetic acid (75%, 60 ml) and stirred overnight. The solvent was evaporated and the residue codistilled with water (3x) and toluene (2x). The crude product was purified by flash-chromatography.

Diethyl (2-(3-(hypoxanthine-9(6*H*)-yl)-2-(2-(diethoxyphosphoryl)ethoxy)propoxy)ethyl) phosphonate (**5**): starting from 6-chloropurine **3**, yield 76%. ^{1}H NMR (DMSO-d_6): 12.30 bs, 1 H (NH); 8.05 s, 1 H (H-8); 8.03 s, 1 H (H-2); 4.31 dd, 1 H, *J*(gem) = 14.3, *J*(1'b, 2') = 4.3 (H-1'b); 4.18 dd, 1 H, *J*(gem) = 14.3, *J*(1'a, 2') = 7.0 (H-1'b); 3.87-4.04 m, 8 H (Et); 3.84 dtd, 1 H, *J*(2',1'a) = 7.0, *J*(2',3'a) = *J*(2',3'b) = 5.0, *J*(2',1'b) = 4.3 (H-2'); 3.64 m, 1 H (H-6'b); 3.54-3.61 m, 2 H (H-4'); 3.51 m, 1 H (H-6'a); 3.42 dd, *J*(gem) = 10.5, *J*(3'b, 2') = 5.0 (H-3'b); 3.39 dd, *J*(gem) = 10.5, *J*(3'a, 2') = 5.1 (H-3'a); 2.06 dt, 2 H, *J*(5',P) = 18.3, *J*(5',4') = 7.3 (H-5'); 1.89 dt, 2 H, *J*(7',P) = 18.3, *J*(7',6') = 7.4 (H-7'); 1.22 t and 1.184 t and 1.182 t, 12 H, *J* = 7.1 (Et). ^{13}C NMR (DMSO-d_6): 156.94 (C-6); 148.80 (C-4); 145.70 (C-2); 141.16 (C-8); 123.87 (C-5); 76.38 (C-2'); 69.70 (C-3'); 65.05 (C-4');

63.96 (C-6'); 61.18 d and 61.17 d and 61.15 d, *J*(C,P) = 6.2 (Et); 44.32 (C-1'); 26.35 d, *J*(C,P) = 136.2 (C-7'); 26.02 d, *J*(C,P) = 137.3 (C-5'); 16.45 d and 16.40 d and 16.39 d, *J*(C,P) = 5.9 (Et). MS (ESI): m/z = 539.3 $[M+H]^+$.

Diethyl (2-(3-(guanine-9(6*H*)-yl)-2-(2-(diethoxyphosphoryl)ethoxy)propoxy)ethyl) phosphonate (**6**): starting from 2-amino-6-chloropurine **4**, yield 98%. ^{1}H NMR (DMSO-d_6): 10.75 s, 1 H (NH); 7.92 s, 1 H (H-8); 6.58 bs, 2 H (NH_2); 4.13 dd, 1 H, *J*(gem) = 14.3, *J*(1'b,2') = 4.2 (H-1'b); 3.88-4.04 m, 9 H (H-1'a and Et); 3.81 dtd, 1H, *J*(2',1'a) = 7.1, *J*(2',3'a) = *J*(2',3'b) = 5.0, *J*(2',1'b) = 4.2 (H-2'); 3.65 m, 1 H (H-6'b); 3.56-3.61 m, 2 H (H-4'); 3.53 m, 1 H (H-6'a); 3.42 dd, 1 H, *J*(gem) = 10.4, *J*(3'b, 2') = 5.0 (H-3'b); 3.38 dd, 1 H, *J*(gem) = 10.4, *J*(3'a, 2') = 5.0 (H-3'a); 2.07 dt, 2 H, *J*(5',P) = 18.3, *J*(5',4') = 7.4 (H-5'); 1.91 dt, 2 H, *J*(7',P) = 18.3, *J*(7',6') = 7.4 (H-7'); 1.22 t and 1.19 t, 12 H, *J* = 7.1 (Et). ^{13}C NMR (DMSO-d_6): 156.39 (C-6); 154.04 (C-2); 151.32 (C-4); 138.30 (C-8); 114.82 (C-5); 76.11 (C-2'); 69.66 (C-3'); 65.00 (C-4'); 63.89 (C-6'); 61.22 d and 61.20 d, *J*(C,P) = 6.1 (Et); 44.07 (C-1'); 26.32 d, *J*(C,P) = 136.3 (C-7'); 26.00 d, *J*(C,P) = 136.9 (C-5'); 16.44 d and 16.39 d, *J*(C,P) = 5.8 (Et). MS (ESI): m/z = 554.1 $[M+H]^+$.

Tetraisopropyl ([(2-((hypoxanthine-9*H*-yl)methyl)propane-1,3-diyl)bis(oxy)]bis(methylene))bis(phosphonate) (**14**): starting from 6-chloropurine **12**, yield 98%. ^{1}H NMR (DMSO-d_6): 12.30 bd, 1 H, *J*(NH,2) = 3.9 (NH); 8.08 s, 1 H (H-8); 8.03 d, 1 H, *J*(2,NH) = 3.9 (H-2); 4.59 dsept, 4 H, *J*(CH,P) = 7.7, *J*(CH,CH_3) = 6.2 (*i*Pr); 4.17 d, 2 H, *J*(1',2') = 7.0 (H-1'); 3.72 dd, 2 H, *J*(gem) = 14.1, *J*(4'b,P) = 8.0 (H-4'b); 3.69 dd, 2 H, *J*(gem) = 14.1, *J*(4'b,P) = 8.0 (H-4'a); 3.49 dd, 2 H, *J*(gem) = 9.8, *J*(3'b,2') = 5.7 (H-3'b); 3.47 dd, 2 H, *J*(gem) = 9.8, *J*(3'a,2') = 5.7 (H-3'a); 2.46 m, 1 H (H-1'); 1.24 d and 1.23 d, 24 H, *J*(CH_3,CH) = 6.2 (*i*Pr). ^{13}C NMR (DMSO-d_6): 156.78 (C-6); 148.70 (C-4); 145.76 (C-2); 140.88 (C-8); 123.95 (C-5); 70.92 d, *J*(C,P)

= 11.2 (C-3'); 70.37 d and 70.35 d, *J*(C,P) = 6.4 (*i*Pr); 65.29 d, *J*(C,P) = 164.1 (C-4'); 42.41 (C-1'); 39.44 (C-2'); 24.02 d and 23.92 d, *J*(C,P) = 3.7 and 4.5 (*i*Pr). MS (ESI): m/z = 581.3 $[M+H]^+$.

Tetraisopropyl ([(2-((guanine-9*H*-yl)methyl)propane-1,3-diyl)bis(oxy)]bis(methylene))bis(phosphonate) (**15**): starting from 2-amino-6-chloropurine **13**, yield 84%. The spectral data were in accord with the literature.[10a]

Synthesis of the free bisphosphonates 7-8 and 16-17 - General procedure

A mixture of tetraesters **5, 6, 14** or **15** (1 mmol), acetonitrile (20 ml) and $BrSiMe_3$ (2 ml) was stirred overnight at room temperature. After evaporation and codistillation with acetonitrile (3x), the residue was stirred with MeOH:water (1:1, 100 ml) for 2 h at room temperature. The solvent was evaporated in vacuo and the residue was purified by preparative HPLC (water–methanol) and the product was obtained after codistillation with methanol as white solid.

(2-(3-(Hypoxanthine -9(6H)-yl)-2-(2-(bishydroxyphosphoryl)ethoxy)propoxy)ethyl) phosphonic acid (**7**): starting from tetraester **5**, yield 55%. ^{1}H NMR (DMSO-d_6): 12.69 bs, 1 H (NH); 8.67 s, 1 H (H-8); 8.18 s, 1 H (H-2); 4.39 dd, 1 H, *J*(gem) = 14.3, *J*(1'a,2') = 4.2 (H-1'a); 4.26 dd, 1 H, *J*(gem) = 14.3, *J*(1'b,2') = 7.0 (H-1'b); 3.84 m, 1 H (H-2'); 3.69 m, 1 H (H-6'a); 3.51-3.61 m, 3 H (H-4' and H-6'b); 3.40-3.47 m, 2 H (H-3'); 1.69-1.90 m, 4 H (H-5' and H-7'). ^{13}C NMR (DMSO-d_6): 155.40 (C-6); 148.17 (C-4); 147.15 (C-2); 141.08 (C-8); 120.37 (C-5); 75.79 (C-2'); 69.48 (C-3'); 65.96 (C-4'); 64.71 (C-6'); 45.21 (C-1'); 29.04 d, *J*(C,P) = 133.8 and 28.83 d, *J*(C,P) = 134.4 (C-5'and C-7'). HR-MS (ESI-) for $C_{12}H_{19}O_9N_4P_2$ calculated: 425.0633, found: 425.0628.

(2-(3-(Guanin-9(6H)-yl)-2-(2-(bishydroxyphosphoryl)ethoxy)propoxy)ethyl)phosphonic acid (**8**): starting from tetraester **6**, yield 62%. ^{1}H NMR (DMSO-d_6): 10.54 s, 1 H (NH); 7.65 s, 1 H (H-8); 6.49 s, 2 H (NH_2); 4.09 dd, 1 H, *J*(gem) = 14.3, *J*(1'b,2') = 4.3 (H-1'b); 3.95 dd, 8 H, *J*(gem) = 14.3, *J*(1'a,2') = 7.2 (H-1'a); 3.75 bdtd, 1H, *J*(2',1'a) = 7.2, *J*(2',3'a) = *J*(2',3'b) = 5.0, *J*(2',1'b) = 4.5 (H-2'); 3.66 m, 1 H (H-6'b); 3.58-3.63 m, 2 H (H-4'); 3.54 m, 1 H (H-6'a); 3.40 dd, 1 H, *J*(gem) = 10.6, *J*(3'b, 2') = 4.8 (H-3'b); 3.35 dd, 1 H, *J*(gem) = 10.6, *J*(3'a, 2') = 5.3 (H-3'a); 1.88 ddd, 2 H, *J*(5',P) = 18.4, *J*(5',4') = 8.0 (H-5'); 1.66-1.75 m, 2 H, *J*(7',P) = 18.4 (H-7'). ^{13}C NMR (DMSO-d_6): 156.91 (C-6); 153.72 (C-2); 151.48 (C-4); 138.38 (C-8); 116.30 (C-5); 76.21 (C-2'); 69.77 (C-3'); 65.92 (C-4'); 64.76 (C-6'); 43.86 (C-1'); 29.22 d, *J*(C,P) = 133.2 (C-7'); 28.94 d, *J*(C,P) = 134.1 (C-5'). HR-MS (ESI-) for $C_{12}H_{20}O_9N_5P_2$ calculated: 440.0742, found: 440.0737.

([(2-((hypoxanthine-9*H*-yl)methyl)propane-1,3-diyl)bis(oxy)]bis(methylene))diphosphonic acid (**16**): starting from tetraester **14**, yield 73%. ^{1}H NMR (DMSO-d_6): 12.31 bs, 1 H (NH); 8.09 s, 1 H (H-8); 8.04 s, 1 H (H-2); 4.18 d, 2 H, *J*(1', 2') = 7.2 (H-1'); 3.54 m, 4 H, *J*(4', P) = 7.8 (H-4'); 3.51 dd, 2 H, *J*(gem) = 9.4, *J*(3'b, 2') = 5.1 (H-3'b); 3.49 dd, 2 H, *J*(gem) = 9.4, *J*(3'a, 2') = 5.8 (H-3'a); 2.40 tpent, 1 H, *J*(2',1') = 7.2, *J*(2',3'a) = *J*(2',3'b) = 5.5 (H-2'). ^{13}C NMR (DMSO-d_6): 156.81 (C-6); 148.70 (C-4); 145.78 (C-2); 141.07 (C-8); 123.95 (C-5); 70.16 d, *J*(C,P) = 8.5 (C-3'); 66.46 d, *J*(C,P) = 160.6 (C-4'); 42.44 (C-1'); 39.79 (C-2'). HR-MS (ESI-) for $C_{11}H_{17}O_9N_4P_2$ calculated: 411.0476, found: 411.0473.

([(2-((guanine-9*H*-yl)methyl)propane-1,3-diyl)bis(oxy)]bis(methylene))diphosphonic acid (PP-P352=SV278)-(**17**): starting from tetraester **15**, yield 68%. The spectral data were in accord with the literature.[10a]

9-[1,3-bis(phosphonomethoxy)propan-2-yl]guanine (20)

This bisphosphonate was prepared according the literature.[10b]

Synthesis of prodrugs of ANPs

Bis *N*-((*S*)-1-ethoxy-1-oxopropan-2-yl) amidate of 9-(2-phosphonomethoxy-3-hydroxypropyl)guanine (21)

Triethylamine (2.0 ml) was added to a suspension of PEEG (1.0 mmol) and L-alanine ethylester hydrochloride (614 mg, 4.0 mmol) in anhydrous pyridine (8 ml). The mixture was heated to 60 °C and a freshly prepared solution of triphenylphosphine (6.0 mmol, 1.57 g) and Aldrithiol (6.0 mmol, 1.32 g) in anhydrous pyridine (12 ml) was added. The mixture was heated to 60 °C for 10 h. The solution was evaporated, codistilled with toluene and the residue was chromatographed on a silica gel column in gradient 20 % MeOH/EtOAc → 20 % MeOH/ $CHCl_3$. Fractions containing product were evaporated. Crude product contaminated with triethylammonium salts was purified on preparative HPLC on XTerra C18 column, 10 mm, 19 × 300 mm, 10 ml/min, mob. phase A: MeOH, mob. phase B: H_2O – MeCN (2:1), gradient: 0 % A (0 min.) → 80 % A (10 min). Fractions containing product were evaporated and the product was crystalized from EtOH – Et_2O, yield 170 mg (34%), m.p. 109-114 °C. Anal. Calcd for $C_{19}H_{34}N_7O_8P$ (monohydrate): C, 43.93; H, 6.60; N, 18.87; P, 5.96. Found: C, 44.18; H, 6.39; N, 18.84; P, 5.68. ^{1}H NMR (DMSO-d_6) : 1.19 t, 3 H, J = 7.1 (Et); 1.21 t, 3 H, J = 7.1 (Et); 1.25-1.28 m, 6 H, (CH_3 Ala); 1.85-1.92 m, 2 H (H-4´); 3.60-3.66 m, 2 H (H-3´); 3.70 t, 2 H, J(2´-1') = 5.5 (H-2´); 3.78-3.87 m, 2 H (CH Ala); 4.03-4.14 m, 7 H (Et and H-1´); 4.30 m, 1 H (NH); 6.27 bs (NH_2); 7.64 s, 1 H (H-8);

10.39 s, 1 H (NH). ^{13}C NMR (DMSO-d_6) : 13.76 (Et); 20.30-20.43 m (CH_3 Ala); 30.00 d, J(4´-P) = 111.3 (C-4´); 42.34 (C-1´); 48.03, 48.06 (CH Ala); 60.10, 60.15 (Et); 64.98 (C-3´); 67.97 (C-2´); 116.47 (C-5); 137.34 (C-8); 151.05 (C-4);, 153.38 (C-2); 156.58 (C-6); 173.82 – 173.90 m (CO). ESI-HRMS calcd for $C_{19}H_{33}N_7O_7P$ 502.21736, found: 502.21732 $[M+H]^+$. ESI-MS, m/z: 502.3 (8) $[M+H]^+$, 524.3 (100) $[M+Na]^+$.

Bis hexadecyloxypropyl ester of PEEG (22) and mono hexadecyloxypropyl ester of PEEG (23)

Bis hexadecyloxypropyl ester of PEEG **22** together with corresponding monoester **23** (**Figure 5**) were prepared according the recently published procedure.[22a]

Synthesis of phosphoramidate prodrugs 9-10 and 18-19 - General procedure

A mixture of bisphosphonic acid tetraester (1 mmol) was codistilled with dry acetonitrile (2x). Dry acetonitrile (20 ml) and bromotrimethylsilane (2 ml) were added and mixture was stirred overnight at room temperature under argon. After evaporation (without any contact with air) in vacuo (40 °C, 20 mbar) and codistillation with dry acetonitrile (3x) (without any contact with air), the flask was purged with argon and ethyl L-phenylalanine hydrochloride (2.5g, 10.88 mmol, dried in vacuo at 30 °C and 0.1 mbar for 1 day), dry triethylamine (5 ml), and dry pyridine (15 ml) were added and this mixture was heated to 60 °C to obtain a homogenous solution and a solution of 2-Aldrithiol (3.4g, 15.4 mmol) and triphenylphosphine (4g, 15.3 mmol) in 15 ml of dry pyridine under argon was added immediately. The resulting mixture was heated at 70 °C for 3 days to reach full conversion. After cooling, the bright yellow solution was evaporated in vacuo and the residue was purified first by flash-chromatography (silica

gel, $CHCl_3$-MeOH gradient 1-10%) and then by preparative HPLC (C18, water-MeOH gradient 0-100%). The product was obtained as colorless / yellowish foam.

tetra-(L-Phenylalanine ethylester)-prodrug of (2-[3-(hypoxanthine -9-yl)-2-(2-(bishydroxyphosphoryl)ethoxy)propoxy]ethyl) phosphonic acid (**9**): starting from tetraester **5**, yield 15%. ^{1}H NMR (DMSO-d_6): 12.31 bs, 1 H (NH); 8.04 s and 8.03 s, 1 H (H-2); 7.93 s and 7.92 s, 1 H (H-8); 7.06-7.30 m, 20 H (Ph); 4.41-4.53 m, 2 H (NH); 3.90-4.21 m, 14 H (H-1' and NH and CH and Et); 3.78-3.91 m, 2 H (CH); 3.53-3.62 m, 1 H (H-2'); 3.21-3.47 m, 4 H (H-6' and H-4'); 3.09-3.21 m, 2 H (H-3'); 2.79-2.94 m and 2.67-2.76 m, 8 H ($\underline{CH_2}$Ph); 1.35-1.67 m, 4 H (H-5' and H-7'); 1.12 t and 1.11 t and 1.06 t and 1.05 t and 1.04 t, 12 H, J = 7.1 (Et). ^{13}C NMR (DMSO-d_6): 173.09-173.31 m (CO); 156.89 and 156.88 (C-6); 148.75 and 148.72 (C-4); 145.62 (C-2); 141.10 (C-8); 137.35-137.47 m (*i*-Bn); 129.56-129.61 m (*o*-Bn); 128.25-128.30 m (*m*-Bn); 126.62-126.68 m (*p*-Bn); 123.82 and 123.81 (C-5); 76.09 and 75.95 (C-2'); 69.28 and 69.23 (C-3'); 65.63 (C-4'); 64.32 (C-6'); 60.43-60.57 m (Et); 53.90-54.38 m (CH); 44.14 and 44.09 (C-1'); 40.1 m ($\underline{C}H_2$Ph); 30.4 m (C-7'); 30.1 m (C-5'); 14.12 and 14.06 (Et). HR-MS (ESI+) for $C_{56}H_{73}O_{13}N_8P_2$ calculated: 1127.4767, found: 1127.4772.

tetra-(L-Phenylalanine ethylester)-prodrug of (2-[3-(guanin-9-yl)-2-(2-(bishydroxyphosphoryl)ethoxy)propoxy]ethyl)phosphonic acid (**10**): starting from tetraester **6**, yield 54%. ^{1}H NMR (DMSO-d_6): 10.55 bs, 1 H (NH); 7.52 s and 7.51 s, 1 H (H-8); 7.10-7.28 m, 20 H (Ar); 6.52 bs and 6.50 bs, 2 H (NH_2); 4.43-4.55 m, 2 H (NH); 4.06-4.16 m, 2 H (NH); 3.81-4.05 m, 14 H ($COOCH_2$, NH-CH, H-1'); 3.51 m, 1 H (H-2'); 3.25-3.41 m, 4 H (H-4' and H-6'); 3.07-3.15 m, 2 H (H-3'); 2.70-2.94 m, 8 H (CH_2Ph); 1.43-1.64 m, 4 H (H-5' and H-7'); 1.04-1.13 m, 12 H (CH_3). ^{13}C NMR (DMSO-d_6): 173.05-173.28 m, (CO); 157.03 and 157.02 (2 x C-6); 153.72 and 153.71 (2 x C-2); 151.63 and 151.62 (2 x C-4); 138.28 and 138.24 (2 x C-8); 137.31-137.46

m, (C-1''); 129.55-129.59 m, (C-2''); 128.25-128.31 m, (C-3''); 126.60-126.69 m, (C-4''); 116.37 and 116.34 (2 x C-5); 75.97 and 75.91 (2 x C-2'); 69.26 and 69.17 (2 x C-3'); 65.47 and 65.42 (2 x C-4'); 64.13 and 64.10 (2 x C-6'); 60.43-60,57 m, (Et); 53.93-53.38 m, (NH-CH); 43.33 and 43.28 (2 x C-1'); 40.09 (CH_2Ph); 29.60-30.75 m, (C-5'and C-7'); 14.04-14.12 m, (CH_3). HR-MS (ESI+) for $C_{56}H_{74}O_{13}N_9P_2$ calculated: 1142.4876, found: 1142.4879.

tetra-(L-Phenylalanine ethylester)-prodrug of ([(2-((hypoxanthine-9*H*-yl)methyl)propane-1,3-diyl)bis(oxy)]bis(methylene))diphosphonic acid (18): starting from tetraester **14**, yield 47%. ^{1}H NMR (DMSO-d_6): 12.29 bs, 1 H (NH); 8.05 s, 1 H (H-8); 7.98 s, 1 H (H-2); 7.12-7.24 m, 20 H (Ar); 4.50-4.58 m, 2 H (NH); 4.18-4.26 m, 2 H (NH); 4.09-4.16 m, 2H, (H-1'); 3.90-4.06 m, 12 H, (NH-CH, Et); 3.07-3.28 m, 8 H (H-3' and CH_2P); 2.77-2.90 m, 8 H (CH_2Ph); 2.23 m, 1 H (H-2'); 1.12 t, 1.11 t, 1.06 t and 1.06 t, 12 H, J = 7.1 (Et). ^{13}C NMR (DMSO-d_6): 172.85-173.09 m, (COO); 156.80 (C-6); 148.63 (C-4); 145.69 (C-2); 141.15 (C-8); 137.25 (C-1''); 129.57-129.60 (C-2''); 128.22 (C-3''); 126.61 (C-4''); 124.00 (C-5); 70.11-70.53 m, (C-3'); 67.07-68.28 m, (CH_2P); 60.61, 60.60 and 60.51 (Et); 54.21, 53.89 and 53.86 (NH-CH); 41.52 (C-1'); 39.90 (CH_2Ph); 39.50 (C-2'); 14.10, 14.09 and 14.03 (CH_3). HR-MS (ESI+) for $C_{55}H_{71}O_{13}N_8P_2$ calculated: 1113.4610, found: 1113.4614.

tetra-(L-Phenylalanine ethylester)-prodrug of ([(2-((guanine-9*H*-yl)methyl)propane-1,3-diyl)bis(oxy)]bis(methylene))diphosphonic acid (19): starting from tetraester **15**, yield 67%. ^{1}H NMR (DMSO-d_6): 10.57 bs, 1 H (NH); 7.63 s, 1 H (H-8); 7.09-7.25 m, 20 H (Ar); 6.42 bs, 2 H (NH_2); 4.43-4.50 m, 2 H (NH); 4.16-4.21 m, 2 H (NH); 3.88-4.05 m, 14 H (H-1', NH-CH, Et); 3.13-3.24 m, 8 H (H-3' and CH_2P); 2.76-2.92 m, 8 H (CH_2Ph); 2.20 m, 1 H (H-2'); 1.02-1.13 m, 12 H (CH_3). ^{13}C NMR (DMSO-d_6): 172.73-172.96 m, (COO); 156.94 (C-6); 153.67 (C-2); 151.45

(C-4); 138.22 (C-8); 137.12-137.27 m, (C-1''); 129.54 (C-2''); 128.19-128.21 m, (C-3''); 126.56-126.61 m, (C-4''); 116.69 (C-5); 70.39-70.59 m, (C-3'); 67.30-68.22 m, (CH_2P); 60.47-60.57 m, (Et); 53.91-54.06 m, (NH-CH); 41.13 (C-1'); 40.07 (CH_2Ph); 39.33 (C-2'); 13.96-14.04 m, (CH_3). HR-MS (ESI+) for $C_{55}H_{72}O_{13}N_9P_2$ calculated: 1128.4719, found: 1128.4726.

Crystallization and structure determination of human HGPRT in complex with compound 17

For crystallization experiments, human HGPRT was concentrated to 11.1 mg/ml (0.44 mM in terms of subunits). After concentration, the enzyme is stored at -70°C in 0.1 M Tris-HCl, 0.01 M $MgCl_2$, 1 mM DTT, 300 mM *P*Rib-*PP,* pH 7.4. Under these conditions, there is no loss of activity for >24 months. Prior to crystallization, the enzyme was incubated with compound **17** for ~five minutes to give a final concentration of the compound of 0.88 mM. For crystallization, the hanging drop method was used where 1 μL of reservoir solution and 1 μL of human HGPRT in complex with the inhibitor were combined in the drops and incubated at 18ºC. The reservoir solution was 0.2 M $LiSO_4$, 30% PEG 5000 MME, 0.1 M Tris-HCl, pH 8.0. Prior to data collection, crystals were transferred to a cryoprotectant solution that contained well solution, 0.8 mM inhibitor and 20% glycerol. These crystals were then placed in a cryostream (100 K). X-ray data were collected using Beamline MX2 of the Australian Synchrotron. Both data sets were scaled and merged using Xds.[25]

The structure was solved by molecular replacement using the program PHASER,[26] within PHENIX 1.7.3[27] and the protein coordinates of the tetramer of human HGPRT in complex with immucillinHP-Mg^{2+}-PP_i (except that the mobile loop residues 102-

127 were removed) as the starting model (PDB code 1BZY). One tetramer could be fitted to the asymmetric unit giving a translation function Z-score of 40.2 and a log likelihood-gain (LLG) of 998 and with no steric clashes. Subsequent refinement of the coordinates was with PHENIX[27] and model building with COOT.[28] The structural restraints file for the inhibitor was generated using the PRODRG2 Dundee server.[29]

The atomic coordinates and structure factors of human HGPRT in complex with compound **17** have been deposited with the Protein Data Bank as entry 4IJQ.

Evaluation of* in vitro *antimalarial activity of ANPs

P. falciparum D6 (Sierra-Leone) laboratory line, sensitive to most antimalarial drugs and W2 (Indochina) line, resistant to chloroquine and pyrimethamine, were maintained in RPMI-1640-LPLF complete medium, containing 10% human plasma, at 4% haematocrit and 1% to 8% parasitaemia as previously described.[30] Cultures were routinely synchronised using D-sorbitol.[31] To evaluate the antimalarial activity of the ANPs the [^{3}H]-hypoxanthine growth inhibition assay[32] was utilised, where the uptake of [^{3}H]-hypoxanthine by malaria parasites is used as a surrogate marker for parasite growth. For these assays, stock solutions of ANPs were made to concentrations of 20-40 mM in DMSO or water and subsequently diluted in hypoxanthine-free complete media prior to assay. The assays (in 96-well plate format) were initiated when the majority of parasites (>90%) were at early trophozoite (ring) stage. Parasite cultures (100 μL per well) at 0.5% initial parasitemia and 2% hematocrit in hypoxanthine-free RPMI1640-LPLF medium were exposed to ten 2-fold serial dilutions of the ANPs and chloroquine (CQ) (reference drug) for 96 hours, with [^{3}H]-hypoxanthine (0.2 μCi/well) added ~48 hours after beginning of the experiment.

The [^{3}H]-hypoxanthine incorporation data were analyzed and sigmoidal growth inhibition curves were produced by non-linear regression analysis of the [^{3}H]-hypoxanthine incorporation data versus log-transformed concentrations of the compounds using Graphpad Prism V5.0 software (GraphPad Software Inc. USA), from which the inhibitory concentration (IC_{50}) that cause 50% of parasite growth were determined. The IC_{50} values were based on three independent experiments with mean ± SD calculated.

Cytotoxicity assays

The inhibitory effect of the test compounds on cell proliferation was determined in three human cell lines (purchased from the American Type Culture Collection): A549 lung carcinoma cells; C32 melanoma cells, and C32-TG mutant cells, which were selected under 6-thioguanine and are deficient in HGPRT activity.[33] Sequence analysis on the HGPRT mRNA isolated from C32-TG demonstrated that its HGPRT deficiency is explained by a deletion of exon 2 (107 bp), causing a frame shift and the formation of an unrelated translation product. To determine the cytostatic effect of the test compounds, the cells were seeded in 96-well plates at 7,500 (A549) or 15,000 (C32 and C32-TG) cells per well and, 24 hr later, the compounds were added at serial dilutions. After four days incubation at 37 °C, the cells were trypsinized and counted with a Coulter Counter apparatus. The CC_{50} values, or compound concentrations at which cell proliferation was 50% compared to that in untreated cells, were calculated by extrapolation. Data presented are the mean ± SEM of two or three independent tests.

Enzyme purification and determination of K_i values

N-terminal hexa-histidine tagged human HGPRT and *Pv*HGPRT were purified to homogeneity using IMAC affinity chromatography as previously reported.[8b] *Pf*HGXPRT was purified using the published procedure. The K_i values for the inhibitors were calculated using Hanes' plots at a fixed concentration of guanine (60 μM) and variable concentration of *P*Rib-*PP* (2-1000 μM) depending on the $K_{m(app)}$. These were measured at one concentration of each inhibitor.

AUTHOR INFORMATION

Corresponding Authors

*Phone: +61 0 33653549 E-mail: luke.guddat@uq.edu.au or

*Phone: +420 220183262 E-mail: hockova@uochb.cas.cz

Notes

The authors declare no competing financial interest.

ACKNOWLEDGMENTS

The authors would like to acknowledge the contribution of Professor Antonin Holý to this project. Preliminary X-ray data were measured at the University of Queensland Remote-Operation Crystallization and X-ray diffraction facility (UQROCX). The final measurements were made at the MX1 beam line, Australian Synchrotron, Clayton, Victoria with the assistance of Alan Riboldi-Tunnicliffe and Tom Caradoc-Davies. The views expressed herein are those of the authors and not necessarily those of the owner or operator of the Australian Synchrotron. The authors wish to thank Wim van Dam and Stijn Stevens for excellent technical assistance with cytotoxicity assays. The authors thank Kerryn Rowcliffe for assistance with drug susceptibility assays and the

Australian Red Cross Blood Service (Brisbane) for providing human erythrocytes and plasma for the *in vitro* cultivation of *P. falciparum* lines. The opinions expressed herein are those of the author's and do not necessarily reflect those of the Australian Defence Force, Joint Health Command or any extant policy. This work was supported by the subvention for development of research organization (Institute of Organic Chemistry and Biochemistry) RVO 61388963, by the Grant Agency of the Czech Republic (grant no. P207/11/0108), by funds from the National Health and Medical Research Council, Australia (Grant nos. 569703 and 1030353) and by Gilead Sciences (Foster City, CA, USA).

ABBREVIATIONS USED

*P*Rib-*PP*, 5-phospho-α-D-ribosyl-1-pyrophosphate; PRTase, phosphoribosyltransferase; HGPRT, hypoxanthine-guanine-phosphoribosltransferase; HGXPRT, hypoxanthine-guanine-xanthine phosphoribosyltransferase; ANP, acyclic nucleoside phosphonate; NP, nucleoside phosphonate; immGP, (1S)-1-(9-deazaguanin-9-yl)-1,4-dideoxy-1,4-imino-D-ribitol 5-phosphate; immHP, (1S)-1-(9-deazahypoxanthin-9-yl)-1,4-dideoxy-1,4-imino-D-ribitol 5-phosphate; PEE, 9-[2-(2-phosphonoethoxy)ethyl]; PEEG, 9-[2-(2-phosphonoethoxy)ethyl]guanine; PEEHx, 9-[2-(2-phosphonoethoxy)ethyl]hypoxanthine *Pf*, *Plasmodium falciparum*; *Pv*, *Plasmodium vivax*; A549, human lung carcinoma cells; C32, a human melanoma cell line; C32TG, a derived HGPRT-deficient mutant cell line; HIV, human immunodeficiency virus; PME, 9-[2-(2-phosphonomethoxy)ethyl]; GMP, guanosine monophosphate; IMP, inosine monophosphate; (*S*)-(HPMPG), (S)-3-hydroxy-2-(phosphonomethoxy)propyl guanine; Hx, hypoxanthine; MME, monomethylether;

DTT, dithiothreitol; DMSO, dimethylsulfoxide ; RPMI1640-LPLF, Roswell Park Memorial Institute 1640, low PABA low folic acid; SEM, standard error of the mean; IMAC, immobilized-metal affinity chromatography

REFERENCES

1. http://www.who.int/malaria/publications/atoz/9789241564106/en/index.html.

2. Snow, R. W.; Guerra, C. A.; Noor, A. M.; Myint, H. Y.; Hay, S. I., The global distribution of clinical episodes of *Plasmodium falciparum* malaria. *Nature* **2005,** *434* (7030), 214-217.

3. Dondorp, A.M.; Fairhurst, R. M.; Slutsker, L.; Macarthur, J.R.; Breman J.G.; Guerin, P.J.; Wellems, T.E.; Ringwald, P.; Newman, R.D.; Plowe, C. V., The threat of artemesinin-resistant malaria. *N. Eng. J. Med.* **2011**, 365(12), 1073-1075.

4. (a) Smeijsters, L. J.; Franssen, F. F.; Naesens, L.; de Vries, E.; Holý, A.; Balzarini, J.; de Clercq, E.; Overdulve, J. P., Inhibition of the *in vitro* growth of *Plasmodium falciparum* by acyclic nucleoside phosphonates. *Int. J. Antimicrob. Agents* **1999,** *12* (1), 53-61; (b) Keough, D. T.; Hocková, D.; Holy, A.; Naesens, L. M.; Skinner-Adams, T. S.; Jersey, J.; Guddat, L. W., Inhibition of hypoxanthine-guanine phosphoribosyltransferase by acyclic nucleoside phosphonates: a new class of antimalarial therapeutics. *J. Med. Chem.* **2009,** *52* (14), 4391-4399.

5. (a) Berg, M.; Van der Veken, P.; Goeminne, A.; Haemers, A.; Augustyns, K., Inhibitors of the purine salvage pathway: a valuable approach for antiprotozoal chemotherapy? *Curr. Med. Chem.* **2010,** *17* (23), 2456-2481; (b) de Jersey, J.; Holý, A.; Hocková, D.; Naesens, L.; Keough, D. T.; Guddat, L. W., 6-oxopurine phosphoribosyltransferase: a target for the development of antimalarial drugs. *Curr. Top. Med Chem.* **2011,** *11* (16), 2085-2102; (c) Hazleton, K. Z.; Ho, M. C.; Cassera, M. B.; Clinch, K.; Crump, D. R.; Rosario, I., Jr.; Merino, E. F.; Almo, S. C.; Tyler, P. C.; Schramm, V. L., Acyclic immucillin phosphonates: second-generation inhibitors of

Plasmodium falciparum hypoxanthine-guanine-xanthine phosphoribosyltransferase. *Chem. Biol.* **2012,** *19* (6), 721-730.

6. Carlton, J. M.; Adams, J. H.; Silva, J. C.; Bidwell, S. L.; Lorenzi, H.; Caler, E.; Crabtree, J.; Angiuoli, S. V.; Merino, E. F.; Amedeo, P.; Cheng, Q.; Coulson, R. M. R.; Crabb, B. S.; del Portillo, H. A.; Essien, K.; Feldblyum, T. V.; Fernandez-Becerra, C.; Gilson, P. R.; Gueye, A. H.; Guo, X.; Kang'a, S.; Kooij, T. W. A.; Korsinczky, M.; Meyer, E. V. S.; Nene, V.; Paulsen, I.; White, O.; Ralph, S. A.; Ren, Q. H.; Sargeant, T. J.; Salzberg, S. L.; Stoeckert, C. J.; Sullivan, S. A.; Yamamoto, M. M.; Hoffman, S. L.; Wortman, J. R.; Gardner, M. J.; Galinski, M. R.; Barnwell, J. W.; Fraser-Liggett, C. M., Comparative genomics of the neglected human malaria parasite *Plasmodium vivax*. *Nature* **2008,** *455* (7214), 757-763.

7. (a) Holý, A., Phosphonomethoxyalkyl analogs of nucleotides. *Curr. Pharm. Des.* **2003,** *9* (31), 2567-2592; (b) De Clercq, E.; Holy, A., Acyclic nucleoside phosphonates: a key class of antiviral drugs. *Nat. Rev. Drug Discov.* **2005,** *4* (11), 928-940.

8. (a) Hocková, D.; Holý, A.; Masojídková, M.; Keough, D. T.; de Jersey, J.; Guddat, L. W., Synthesis of branched 9-[2-(2-phosphonoethoxy)ethyl]purines as a new class of acyclic nucleoside phosphonates which inhibit *Plasmodium falciparum* hypoxanthine-guanine-xanthine phosphoribosyltransferase. *Bioorg. Med. Chem.* **2009,** *17* (17), 6218-6232; (b) Keough, D. T.; Hocková, D.; Krečmerová, M.; Česnek, M.; Holý, A.; Naesens, L.; Brereton, I. M.; Winzor, D. J.; de Jersey, J.; Guddat, L. W., *Plasmodium vivax* hypoxanthine-guanine phosphoribosyltransferase: a target for anti-malarial chemotherapy. *Mol. Biochem. Parasitol.* **2010,** *173* (2), 165-169; (c) Krečmerová, M.; Budesinsky, M.; Masojídková, M.; Holý, A., Synthesis of optically active N-6-alkyl derivatives of (R)-3-(adenin-9-yl)-2-hydroxypropanoic acid and

related compounds. *Collect. Czech. Chem. Commun.* **2003,** *68* (5), 931-950; (d) Česnek, M.; Hocková, D.; Holý, A.; Dračínský, M.; Baszczyňski, O.; de Jersey, J.; Keough, D. T.; Guddat, L. W., Synthesis of 9-phosphonoalkyl and 9-phosphonoalkoxyalkyl purines: evaluation of their ability to act as inhibitors of *Plasmodium falciparum*, *Plasmodium vivax* and human hypoxanthine-guanine-(xanthine) phosphoribosyltransferases. *Bioorg. Med. Chem.* **2012,** *20* (2), 1076-1089; (e) Hocková, D.; Keough, D. T.; Janeba, Z.; Wang, T. H.; de Jersey, J.; Guddat, L. W., Synthesis of novel N-branched acyclic nucleoside phosphonates as potent and selective inhibitors of human, *Plasmodium falciparum* and *Plasmodium vivax* 6-oxopurine phosphoribosyltransferases. *J. Med. Chem.* **2012,** *55* (13), 6209-6223.

9. (a) Mackman, R. L.; Cihlar, T., Prodrug strategies in the design of nucleoside and nucleotide antiviral therapeutics. *Ann. Rep. Med. Chem.* **2004,** *39*, 305-321; (b) Hecker, S. J.; Erion, M. D., Prodrugs of phosphates and phosphonates. *J. Med. Chem.* **2008,** *51* (8), 2328-2345.

10. (a) Vrbková, S.; Dračínský, M.; Holý, A., Bifunctional acyclic nucleoside phosphonates: 2. Symmetrical 2-{[bis(phosphono)methoxy]methyl}ethyl derivatives of purines and pyrimidines. *Collect. Czech. Chem. Commun.* **2007,** *72* (7), 965-983; (b) Vrbovská, S.; Holy, A.; Pohl, R.; Masojídková, M., Bifunctional acyclic nucleoside phosphonates. 1. Symmetrical 1,3-bis[(phosphonomethoxy) propan-2-yl] derivatives of purines and pyrimidines. *Collect. Czech. Chem. Commun.* **2006,** *71* (4), 543-566.

11. (a) Hocková, D.; Hocek, M.; Dvořáková, H.; Votruba, I., Synthesis and cytostatic activity of nucleosides and acyclic nucleoside analogues derived from 6-(trifluoromethyl)purines. *Tetrahedron* **1999,** *55* (36), 11109-11118; (b) Corporation, F. Glycerophosphoric acid ester derivative having polyfunctional metal chelate structure, Patent EP1795208 A1. 2007; (c) Baszczynski, O.; Jansa, P.; Dracinsky, M.; Kaiser,

M. M.; Spacek, P.; Janeba, Z., An efficient oxa-Michael addition to diethyl vinylphosphonate under mild reaction conditions. *Rsc Adv* **2012,** *2* (4), 1282-1284.

12. (a) Mitsunobu, O., The use of diethyl azodicarboxylate and triphenylphosphine in synthesis and transformation of natural products. *Synthesis* **1981,** (1), 1-28; (b) Ludek, O. R.; Meier, C., Synthesis of carbocyclic pyrimidine nucleosides, III. Influence of the *N*3-protection group on *N*1-vs. O^2-alkylation in the Mitsunobu reaction. *Eur. J. Org. Chem.* **2006,** (4), 941-946.

13. Zhou, D.; Lagoja, I. M.; Van Aerschot, A.; Herdewijn, P., Synthesis of aminopropyl phosphonate nucleosides with purine and pyrimidine bases. *Collect. Czech. Chem. Commun.* **2006,** *71* (1), 15-34.

14. Jansa, P.; Baszczynski, O.; Dracinsky, M.; Votruba, I.; Zidek, Z.; Bahador, G.; Stepan, G.; Cihlar, T.; Mackman, R.; Holý, A.; Janeba, Z., A novel and efficient one-pot synthesis of symmetrical diamide (bis-amidate) prodrugs of acyclic nucleoside phosphonates and evaluation of their biological activities. *Eur. J. Med. Chem.* **2011,** *46* (9), 3748-3754.

15. Shi, W.; Li, C. M.; Tyler, P. C.; Furneaux, R. H.; Cahill, S. M.; Girvin, M. E.; Grubmeyer, C.; Schramm, V. L.; Almo, S. C., The 2.0 Å structure of malarial purine phosphoribosyltransferase in complex with a transition-state analogue inhibitor. *Biochemistry* **1999,** *38* (31), 9872-9880.

16. Eads, J. C.; Scapin, G.; Xu, Y.; Grubmeyer, C.; Sacchettini, J. C., The crystal structure of human hypoxanthine-guanine phosphoribosyltransferase with bound GMP. *Cell* **1994,** *78* (2), 325-334.

17. Keough, D. T.; Skinner-Adams, T.; Jones, M. K.; Ng, A. L.; Brereton, I. M.; Guddat, L. W.; de Jersey, J., Lead compounds for antimalarial chemotherapy: purine

base analogs discriminate between human and *P. falciparum* 6-oxopurine phosphoribosyltransferases. *J. Med. Chem.* **2006,** *49* (25), 7479-7486.

18. Shi, W.; Li, C. M.; Tyler, P. C.; Furneaux, R. H.; Grubmeyer, C.; Schramm, V. L.; Almo, S. C., The 2.0 Å structure of human hypoxanthine-guanine phosphoribosyltransferase in complex with a transition-state analog inhibitor. *Nat. Struct. Biol.* **1999,** *6* (6), 588-593.

19. Xu, Y.; Eads, J.; Sacchettini, J. C.; Grubmeyer, C., Kinetic mechanism of human hypoxanthine-guanine phosphoribosyltransferase: rapid phosphoribosyl transfer chemistry. *Biochemistry* **1997,** *36* (12), 3700-3712.

20. Keough, D. T.; Brereton, I. M.; de Jersey, J.; Guddat, L. W., The crystal structure of free human hypoxanthine-guanine phosphoribosyltransferase reveals extensive conformational plasticity throughout the catalytic cycle. *J. Mol. Biol.* **2005,** *351* (1), 170-181.

21. (a) Vos, S.; de Jersey, J.; Martin, J. L., Crystal structure of *Escherichia coli* xanthine phosphoribosyltransferase. *Biochemistry* **1997,** *36* (14), 4125-4134; (b) Guddat, L. W.; Vos, S.; Martin, J. L.; Keough, D. T.; de Jersey, J., Crystal structures of free, IMP-, and GMP-bound *Escherichia coli* hypoxanthine phosphoribosyltransferase. *Protein Sci.* **2002,** *11* (7), 1626-1638.

22. (a) Tichý, T.; Andrei, G.; Snoeck, R.; Balzarini, J.; Dračínský, M.; Krečmerová, M., Synthesis and antiviral activities of hexadecyloxypropyl prodrugs of acyclic nucleoside phosphonates containing guanine or hypoxanthine and a (S)-HPMP or PEE acyclic moiety. *Eur. J. Med. Chem.* **2012,** *55*, 307-314; (b) Cheng, X.; He, G.; Lee, W. A.; Wang, J.; Yang, Z.; Rohloff, J. C.; Kim, C. U.; Doerffler, E.; Cook, G. P.; Desai, M. C. Phosphonates, monophosphonamidates, bisphophonamidates for the treatment of viral diseases. Patent WO2005/66189 A1. 2005.

23. Hostetler, K. Y., Alkoxyalkyl prodrugs of acyclic nucleoside phosphonates enhance oral antiviral activity and reduce toxicity: Current state of the art. *Antiviral Res.* **2009,** *82* (2), A84-A98.

24. Birkus, G.; Kutty, N.; Frey, C. R.; Shribata, R.; Chou, T.; Wagner, C.; McDermott, M.; Cihlar, T., Role of cathepsin A and lysosomes in the intracellular activation of novel antipapillomavirus agent GS-9191. *Antimicrob. Agents Chemother.* **2011,** *55* (5), 2166-2173.

25. Kabsch, W., Xds. *Acta Cryst. D* **2010,** *66*, 125-132.

26. McCoy, A. J.; Grosse-Kunstleve, R. W.; Adams, P. D.; Winn, M. D.; Storoni, L. C.; Read, R. J., Phaser crystallographic software. *J. Appl. Cryst.* **2007,** *40*, 658-674.

27. Adams, P. D.; Afonine, P. V.; Bunkoczi, G.; Chen, V. B.; Davis, I. W.; Echols, N.; Headd, J. J.; Hung, L. W.; Kapral, G. J.; Grosse-Kunstleve, R. W.; McCoy, A. J.; Moriarty, N. W.; Oeffner, R.; Read, R. J.; Richardson, D. C.; Richardson, J. S.; Terwilliger, T. C.; Zwart, P. H., PHENIX: a comprehensive Python-based system for macromolecular structure solution. *Acta Cryst. D* **2010,** *66*, 213-221.

28. Emsley, P.; Lohkamp, B.; Scott, W. G.; Cowtan, K., Features and development of Coot. *Acta Cryst. D* **2010,** *66*, 486-501.

29. Schuttelkopf, A. W.; van Aalten, D. M. F., PRODRG: a tool for high-throughput crystallography of protein-ligand complexes. *Acta Cryst. D* **2004,** *60*, 1355-1363.

30. Trager, W.; Jensen, J. B., Human malaria parasites in continuous culture. *Science* **1976,** *193* (4254), 673-675.

31. Lambros, C.; Vanderberg, J. P., Synchronization of *Plasmodium falciparum* erythrocytic stages in culture. *J. Parasitol.* **1979,** *65* (3), 418-420.

32. Desjardins, R. E.; Canfield, C. J.; Haynes, J. D.; Chulay, J. D., Quantitative assessment of anti-malarial activity in vitro by a semiautomated microdilution technique. *Antimicrob. Agents and Chemother.* **1979,** *16* (6), 710-718.

33. Chen, T. R., Chromosome changes in 6-TG-resistant mutant strains derived from a karyotypically stable human line, C32. *Cytogenet. Cell Genet.* **1983,** *35* (3), 181-189.

Table 1. K_i values for bisphosphonate inhibitors of human, *Pf* and *Pv* 6-oxopurine PRTases.

compound[a]	K_i (μM)		
	Human HGPRT	*Pf*HGXPRT	*Pv*HGPRT
17	0.03 ± 0.002	0.07 ± 0.01	0.6 ± 0.07
16	1 ± 0.1	5 ± 1	2 ± 0.3
8	0.6 ± 0.02	0.5±0.01	0.7 ± 0.02
20	37 ± 1	2 ± 0.1	18 ± 2

[a]see **Schemes 1** and **2**; **Figure 3**

Table 2. Data collection and refinement statistics for the human HGPRT.compound **17** complex

Crystal parameters	
Unit cell length *a, b, c* (Å)	56.51, 127.74, 64.76
Unit cell angle α, β, γ (°)	90.0,102.01,90.0
Space group	$P2_1$
Crystal dimensions (mm)	0.4 x 0.1 x 0.05
Diffraction data[a]	
Resolution range (Å)	19.87 - 2.00 (2.11 - 2.00)[a]
Observations	210,171 (27,596)
Unique reflections	59,187 (8,142)
Completeness (%)	98.3 (93.1)
[b]R_{merge}	0.102 (0.784)
[c]$R_{p.i.m.}$	0.054 (0.415)
<I>/<σ(I)>	11.6 (2.7)
Subunits per asym.unit	4
Solvent content (%)	47
Matthews coefficient (Å^3/Da)	2.31
Refinement	
Resolution limits (Å)	19.87 - 2.00 (2.08 - 2.00)
R_{work}	0.1734 (0.2772)
R_{free}	0.2226 (0.3225)

RMSD bond lengths (Å)	0.014
RMSD angles (^{o})	1.29
[d]Clashscore	20.4
Components of the asymmetric unit	
Protein	Subunit A 4-102, 121-217
	Subunit B 4-102,113-217
	Subunit C 5-102,117-217
	Subunit D 4-101,114-217
Inhibitors	4
Water	351
Sulphate	4
Mg^{2+}	8
Ramachandran plot (%)	
Favoured	98.1
Outliers	0.0

[a]Values in parentheses are for the outer resolution shell.

[b]$R_{merge} = \sum_{hkl}\sum_i \left|I_i(hkl) - \left(I(hkl)\right)\right| / \sum_{hkl}\sum_i I_i(hkl)$

[c]$R_{p.i.m.} = \sum_{hkl} \left[\frac{1}{[N(hkl)-1]}\right]^{1/2} \sum_i \left|I_i(hkl) - \left(I(hkl)\right)\right| / \sum_{hkl}\sum_i I_i(hkl)$

where $I_i(hkl)$ is the observed intensity and is the average intensity obtained from multiple observations of symmetry related reflections. [d]Clashscore is defined as the number of bad overlaps ≥ 0.4 Å per thousand atoms.

Table 3. Antimalarial activity and cytotoxicity of PEEG and PEEG prodrugs in cell culture assays

compound	IC_{50} (μM)		CC_{50} (μM)			SI[a]
	D6[b]	W2[c]	A549[d]	C32[e]	C32TG[f]	
PEEG	242	NA[g]	>300	>300	>300	>1
21	42 ± 2	48 ± 2	>300	>300	>300	>7
22	59 ± 9	68 ± 19	>300	>300	>300	>7
23	7.6 ± 1	4.7 ± 3	61 ± 11	61 ± 22	36 ± 1	10
CQ[h]	0.017±0.0006	0.29±0.07				

[a]Estimated selectivity index (SI): average CC_{50} for A549 and C32 cells, divided by the average IC_{50} for *Pf* in red blood cell culture. [b]*Pf* strain sensitive to most drugs; [c]chloroquine- and pyrimethamine- resistant *Pf* strain. [d]Human lung carcinoma cells. [e]Human melonoma cells. [f]Thio-guanine resistant and HGPRT-deficient mutant of the C32 cell line. [g]NA = not attainable *i.e.* no inhibition could be observed. [h]CQ = chloroquine.

Table 4. Antimalarial activity and cytotoxicity of bisphosphonate **17** and prodrugs of the bisphosphonates in cell culture assays.

compound[a]	IC_{50} (μM)		CC_{50} (μM)			SI[b]
	D6[c]	W2[d]	A549[e]	C32[f]	C32TG[g]	
17	NA[i]	NA[i]	>300	>300	>300	>1
19	9.7 ± 1.6	7.1 ± 2.1	>300	130 ± 15	109 ± 8	>18
18	3.8 ± 0.5	4.0 ± 0.9	101 ± 17	41 ± 6	55 ± 4	18
10	6.6 ± 2.3	7.7 ± 1.4	107 ± 55	48 ± 2	46 ± 4	11

[a]**Schemes 1** and **2**; **Figure 6**. [b]Estimated selectivity index (SI): average CC_{50} for A549 and C32 cells, divided by the average IC_{50} for *Pf* in red blood cell culture. [c]Wild-type *Pf* strain sensitive to most drugs; [d]chloroquine- and pyrimethamine- resistant *Pf* strain. [e]Human lung carcinoma cells. [f]Human melonoma cells. [g]Thio-guanine resistant and HGPRT-deficient mutant of the C32 cell line. [h]The produgs of the parent compounds in **Table 1**.[i]NA = not attainable *i.e.* no inhibition could be observed.

FIGURE LEGENDS.

Figure 1. The reaction catalyzed by 6-oxopurine PRTases. The naturally occurring purine bases are guanine (R = $-NH_2$), hypoxanthine (R = -H) and xanthine (R = -OH).

Figure 2. Structure of 2-(phosphonoethoxy)ethyl (PEE) compounds. PEEG: R= $-NH_2$ (guanine); PEEHx: R= -H (hypoxanthine).

Figure 3. Chemical structure of four ANPs in **Table 1** containing a second phosphonate group.

Figure 4. Crystallographic images of the human HGPRT.compound 17 complex. (a) Tetramer of human HGPRT with all four active sites filled with compound 17, two Mg^{2+} and one SO_4^{2-}. (b) Omit unweighted F_o-F_c electron density for compound 17 in subunit A contoured at 3σ. (c) Stereoimage of the interactions between compound 17 and human HGPRT. Water molecules that form hydrogen bonds to compound 17 and the coordination sphere for the Mg^{2+} (pink spheres) are also presented. The SO_4^{2-} is shown as a stick model with the sulfur atom coloured yellow. (d) Stereoimage of the superimposition of the human HGPRT.compound **17** complex (brown) and the human HGPRT.PEEG complex (protein data bank coordinates 3GEP) (cyan).

Figure 5. Structures of the lipophilic prodrugs of PEEG in **Table 3**.

Figure 6. Chemical structures of the prodrugs in **Table 4**.

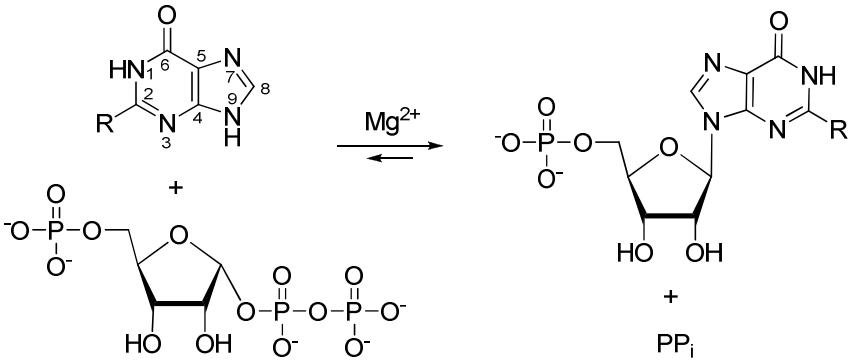

Figure 1.

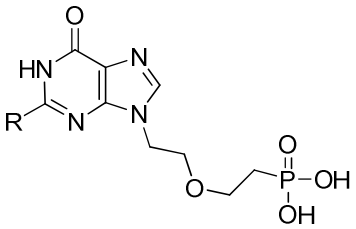

Figure 2.

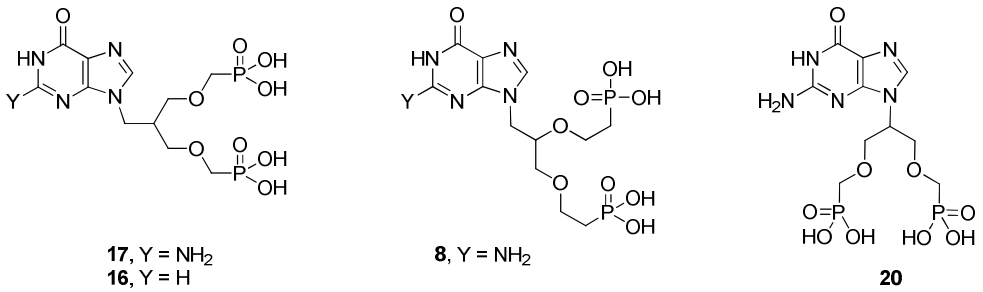

Figure 3.

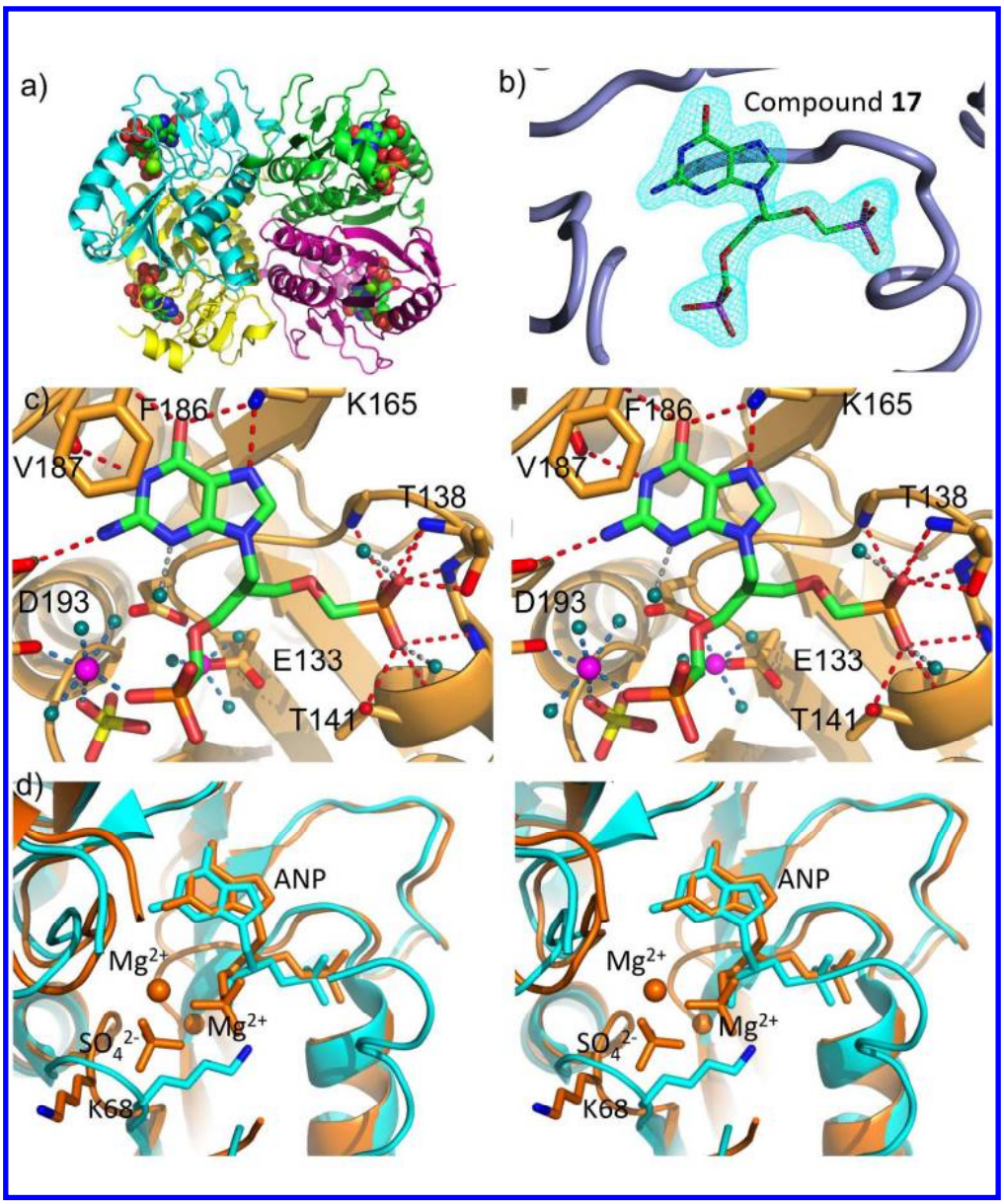
a)
b)
Compound 17
c)
F186
K165
V187
T138
D193
E133
T141
F186
K165
V187
T138
D193
E133
T141
d)
ANP
Mg2+
Mg2+
SO42-
K68
ANP
Mg2+
Mg2+
SO42-
K68

Figure 4.

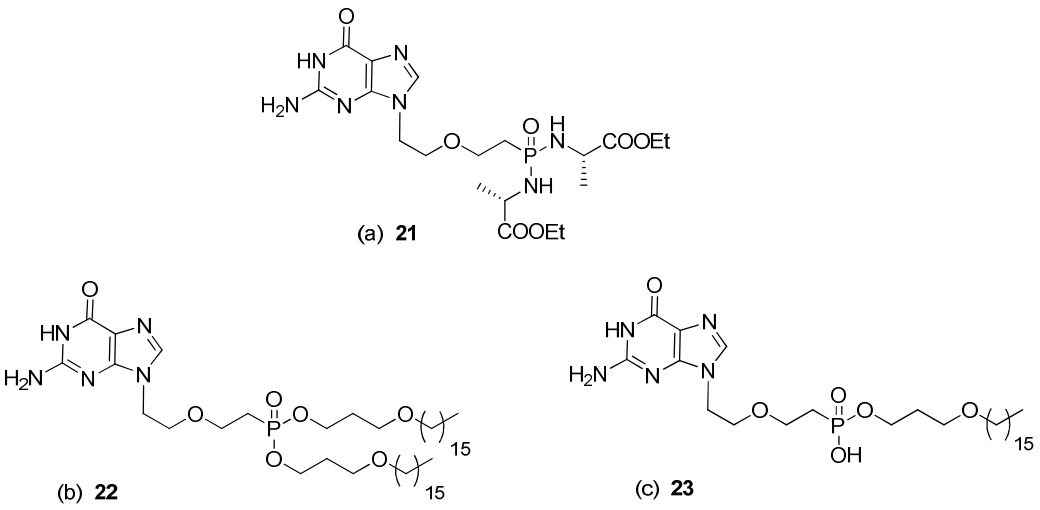

Figure 5.

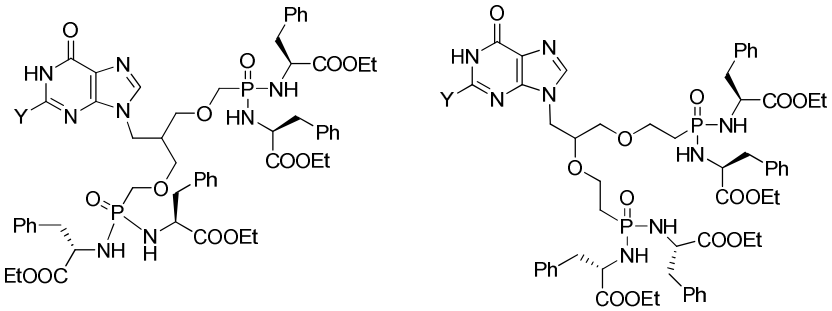

19: Y = NH_2 (prodrug of **17**)
18: Y = H (prodrug of **16**)

10: Y = NH_2 (prodrug of **8**)

Figure 6.

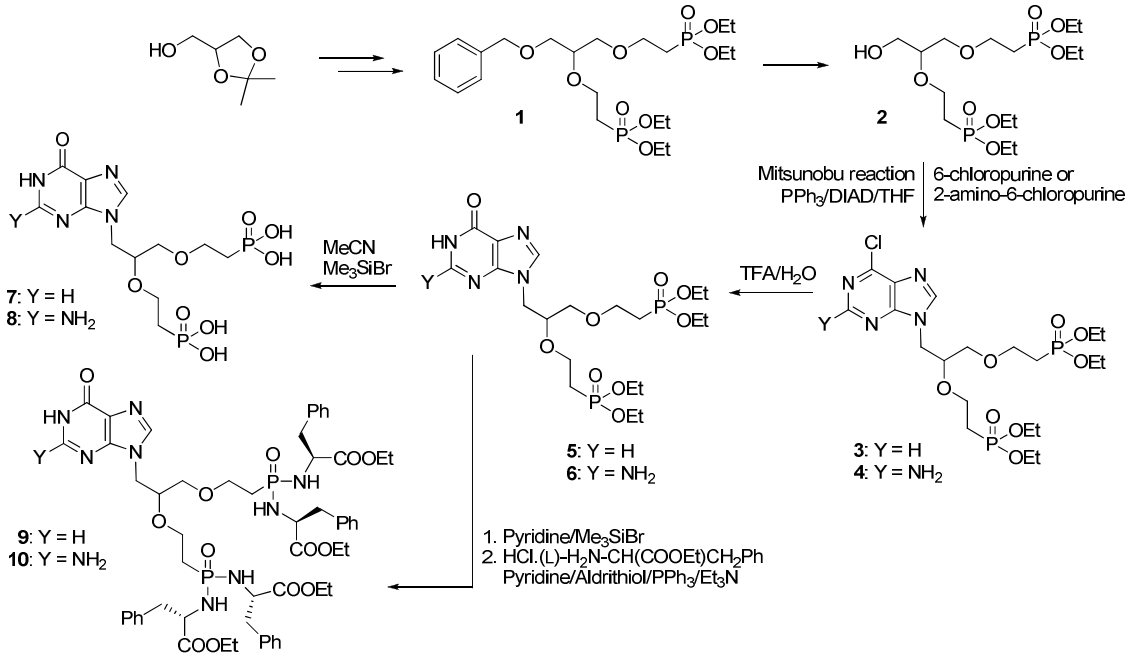
HO
1
2
Mitsunobu reaction
PPh3/DIAD/THF
6-chloropurine or
2-amino-6-chloropurine
TFA/H2O
MeCN
Me3SiBr
7: Y = H
8: Y = NH2
5: Y = H
6: Y = NH2
3: Y = H
4: Y = NH2
9: Y = H
10: Y = NH2
1. Pyridine/Me3SiBr
2. HCl.(L)-H2N-CH(COOEt)CH2Ph
Pyridine/Aldrithiol/PPh3/Et3N

Scheme 1

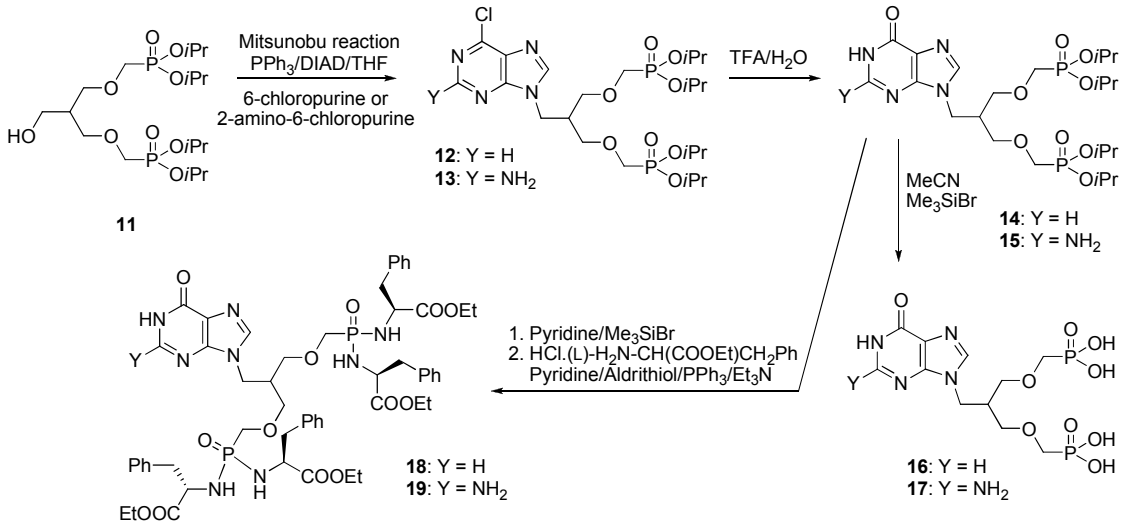
Mitsunobu reaction
PPh3/DIAD/THF
6-chloropurine or
2-amino-6-chloropurine
11
12: Y = H
13: Y = NH2
TFA/H2O
MeCN
Me3SiBr
14: Y = H
15: Y = NH2
16: Y = H
17: Y = NH2
1. Pyridine/Me3SiBr
2. HCl.(L)-H2N-CH(COOEt)CH2Ph
Pyridine/Aldrithiol/PPh3/Et3N
18: Y = H
19: Y = NH2

Scheme 2

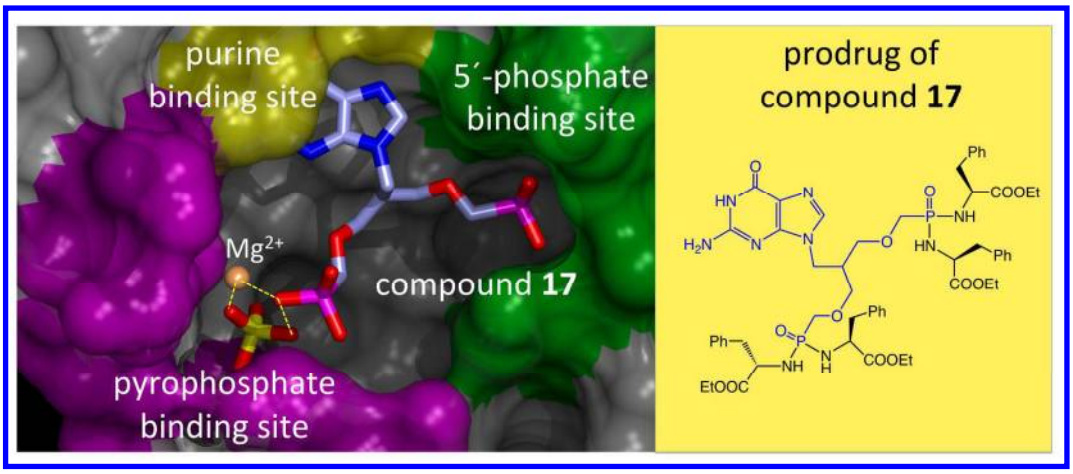

Table of contents graphics